

Analytic Study of Families of Spurious Minima in Two-Layer ReLU Neural Networks

Yossi Arjevani
NYU

yossi.arjevani@gmail.com

Michael Field
UCSB

mikefield@gmail.com

Abstract

We study the optimization problem associated with fitting two-layer ReLU neural networks with respect to the squared loss, where labels are generated by a target network. We make use of the rich symmetry structure to develop a novel set of tools for studying families of spurious minima. In contrast to existing approaches which operate in limiting regimes, our technique directly addresses the nonconvex loss landscape for a finite number of inputs d and neurons k , and provides analytic, rather than heuristic, information. In particular, we derive analytic estimates for the loss at different minima, and prove that modulo $O(d^{-1/2})$ -terms the Hessian spectrum concentrates near small positive constants, with the exception of $\Theta(d)$ eigenvalues which grow linearly with d . We further show that the Hessian spectrum at global and spurious minima coincide to $O(d^{-1/2})$ -order, thus challenging our ability to argue about statistical generalization through local curvature. Lastly, our technique provides the exact *fractional* dimensionality at which families of critical points turn from saddles into spurious minima. This makes possible the study of the creation and the annihilation of spurious minima using powerful tools from equivariant bifurcation theory.

One of the outstanding conundrums of deep learning concerns the ability of simple gradient-based methods to successfully train neural networks despite the nonconvexity of the associated optimization problems. Indeed, generic nonconvex optimization landscapes can exhibit wide and flat basins of attraction around poor local minima which may lead to a complete failure of such methods. The nature by which nonconvex problems associated with neural networks deviate from generic ones is currently not well-understood. In particular, much of the dynamics of gradient-based methods follows from the curvature of the loss landscape around local minima. It is therefore vital to study the local geometry of spurious (i.e., non-global local) and global minima in order to understand the mysterious mechanism which drives gradient-based methods towards minima of high quality. However, already establishing the very existence of spurious minima seems to be beyond reach of existing analytic tools; let alone rigorously arguing about their height, curvature and structure—the aim of this work.

In this paper, we focus on two-layer ReLU neural networks of the form

$$\sum_{i=1}^k \alpha_i \varphi(\langle \mathbf{w}_i, \mathbf{x} \rangle), \quad W \in M(k, d), \quad \boldsymbol{\alpha} \in \mathbb{R}^k, \quad (1)$$

where $\varphi(z) = \max\{0, z\}$ is the ReLU activation function acting entry-wise, $M(k, d)$ denotes the space of $k \times d$ matrices and \mathbf{w}_i denotes the i th row of W . We are primarily interested in characterizing various optimization-related obstructions for local search method, independently of the expressive power of two-layer ReLU networks. Thus, data is understood to be fully realizable. Concretely, we assume that there are d inputs which are drawn from the standard multivariate Gaussian distribution and are labeled by a *planted* target network. We consider directly optimizing the expected squared loss, resulting in the following highly nonconvex optimization problem:

$$\mathcal{L}(W, \boldsymbol{\alpha}) := \frac{1}{2} \mathbb{E}_{\mathbf{x} \sim \mathcal{N}(\mathbf{0}, I_d)} \left[\left(\sum_{i=1}^k \alpha_i \varphi(\langle \mathbf{w}_i, \mathbf{x} \rangle) - \sum_{i=1}^d \beta_i \varphi(\langle \mathbf{v}_i, \mathbf{x} \rangle) \right)^2 \right], \quad (2)$$

where k denotes the number of hidden neurons, $W \in M(k, d)$ and $\alpha_i \in \mathbb{R}^k$ are the optimization variables, and \mathbf{v}_i and β_i are fixed parameters. This setting, in which the data distribution is regulated rather than being allowed to admit worst-case behavior, has drawn a considerable amount of interest in recent years [64, 16, 18, 38, 59, 10, 23, 52, 3], in part due to the growing number of evidences which indicate that any explanation for the empirical success of deep learning (DL) must take into account the intricate interplay between the network architecture, the input distribution and the label distribution (cf. [10, 8, 57] and references therein for hardness results of optimization and learnability under partial sets of assumptions). Moreover, as demonstrated later in the paper, in spite of its apparent simplicity, nonconvex problem (2) shares a few important characteristics with full-scale neural networks, such as low-dimensional minima and extremely skewed Hessian spectrum.

Learning problem (2) has also been studied in the statistical physics community, starting from the 80' and the 90' [22, 55, 35, 60, 17, 7, 50, 51, 49] under the student-teacher (ST) framework, in which one aims to adjust a *student* network so as to fit the output of a *teacher* network. The ST framework offers a clean venue for analyzing optimization-related aspects of neural network models in the spirit of physical reductionism. The success of DL models in the past decade has reinitiated a surge of interest in this framework, e.g., [6, 27, 40, 45]. However, despite the long tradition in the statistical physics community and the wide effort put nowadays by the machine learning community, the perplexing geometry of problem (2) still seems to be out of reach of existing analytic tools in regimes encountered in practice. In this paper, we present a novel set of symmetry-based tools which allows us, for the first time, to analytically characterize various important aspects of the associated highly nonconvex landscape for a finite number of inputs and neurons.

Our contributions, in order of appearance, can be stated as follows:

- We demonstrate that, empirically, and in a well-defined sense, minima in two-layer ReLU neural networks *break* the symmetry of the target weight matrix. Although ReLU networks have been studied for many years, this phenomenon of symmetry breaking seems to have gone largely unnoticed.
- We show that symmetry breaking makes it possible to derive *analytic* expressions for families of spurious minima in the form of *fractional* power series in terms of d and k . Crucially, in contrast to existing approaches which employ various limiting processes, e.g., [6, 27, 40, 45, 28, 41, 12, 32, 13], our method operates in the natural regime where d and k are finite.
- We develop a novel technique which yields an analytic characterization of the Hessian spectrum of minima to $O(d^{-1/2})$ -order for $d \geq k$, and determine the exact *fractional* value of d at which critical

points turn from saddles into spurious minima and back—a key ingredient in understanding how over-parameterization annihilates spurious minima.

- Based on the unique access to high-dimensional spectral information, we closely examine a number of hypotheses in the machine learning literature pertaining to curvature, optimization and generalization. In particular, we prove that the Hessian spectrum at minima concentrates near small positive constants, with the exception of $\Theta(d)$ eigenvalues which grow linearly with d . Although this phenomenon of extremely skewed spectrum has been observed many times [9, 36, 53, 54], to our knowledge, this is the first time it has been established *rigorously* for two-layer ReLU networks. In addition, our analysis shows that the Hessian spectra of spurious and global minima are identical to $O(d^{-1/2})$ -terms, and further implies that the inductive bias of stochastic gradient descent (SGD), provably, can not be exclusively explained in terms of local curvature [31, 34, 33, 61, 62, 11, 15].

The results presented in the paper are threefold: identifying a symmetry breaking principle for two-layer ReLU networks, analytically characterizing spurious minima, and computing the Hessian spectrum. The next three sections are organized accordingly, along with a literature survey of related work. The last section is devoted for a high-level description of the novel symmetry-based technique used in this work. Proofs, formalities and lengthy technical details are deferred to the appendix.

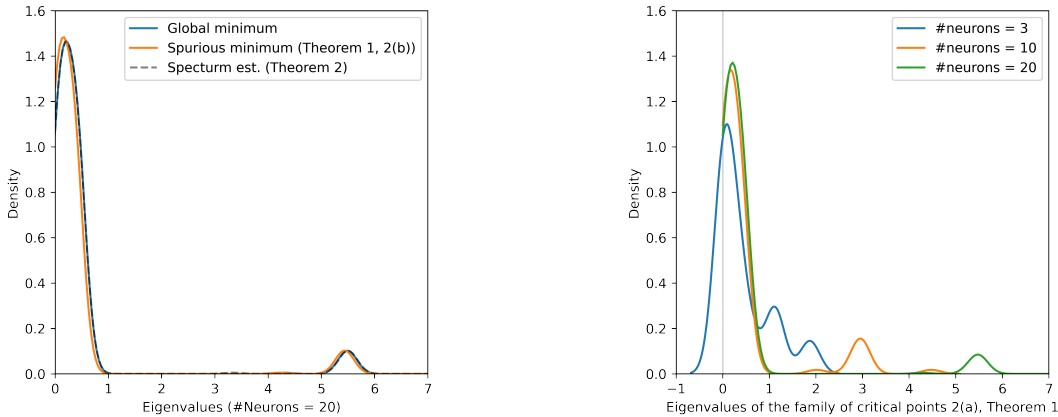


Figure 1: (Left) Our symmetry-based technique yields an *analytic* characterization of the Hessian spectrum (see [Theorem 2](#)) to $O(d^{-1/2})$ -order (in a dashed line) which provides a good approximation already for small values of inputs and neurons (in solid lines). The analysis further implies that the Hessian spectrum of global and various types of spurious minima agree to within $O(d^{-1/2})$ -accuracy. (Right) the Hessian spectrum is extremely skewed and tends to concentrate near small positive constants with the exception of $\Theta(d)$ eigenvalues which grow linearly with d . Observe that the family of critical points considered here (see [Theorem 1](#), case 2a) turns from saddles at $d = 3$ into spurious minima when $d \geq 10$. Our analysis shows that the change of stability occurs at $d \approx 5.71$, and more importantly, indicates that the process can in fact be reversed, namely, spurious minima can be turned into saddles by over-parameterizing (i.e., increasing the number of hidden neurons).

1 Symmetry breaking in two-layer ReLU neural networks

Optimization problem (2) exhibits a very rich symmetry structure. Indeed, the loss function \mathcal{L} is invariant to left- and right-multiplication of W by permutation matrices (see Section A.1 for a formal proof), i.e., $\mathcal{L}(W, \alpha) = \mathcal{L}(P_\pi W P_\rho^\top, \alpha)$ for all $(\pi, \rho) \in S_k \times S_d$, where S_m generally denotes the symmetric group of degree m , and

$$(P_\pi)_{ij} = \begin{cases} 1 & i = \pi(j), \\ 0 & \text{o.w.} \end{cases}.$$

It is therefore natural to ask how the critical points of \mathcal{L} reflect this symmetry. For example, the identity matrix I_d , one of the global minimizers of \mathcal{L} for the case in which $V = I_d$, $\alpha = \beta = \mathbf{1}_d$ and $k = d$, is invariant under *simultaneous* left- and right-multiplication by any permutation matrix. Indeed, $P_\pi I_d P_\pi^\top = P_\pi P_\pi^\top = I_d$ for any $\pi \in S_d$. (Modulo group conjugation, this holds for any global minimizer of \mathcal{L} . See [4, Proposition 4.14].) This simple observation is conveniently stated using the concept of the *isotropy* group defined by

$$\text{Iso}(W) := \{(\pi, \rho) \mid (\pi, \rho) \in S_k \times S_d, P_\pi W P_\rho^\top = W\}, \quad (3)$$

for a given weight matrix W . Thus, we have $\text{Iso}(I_d) = \Delta S_d$, where Δ maps any subgroup $H \subseteq S_d$ to its diagonal counterpart group $\Delta H := \{(h, h) \mid h \in H\} \subseteq S_d \times S_d$. Empirically, and somewhat miraculously, spurious minima and saddles of \mathcal{L} tend to be highly symmetric in the (formal) sense that their isotropy groups are (conjugated to) large subgroups of ΔS_d , the isotropy of the global minima (see Figure 2). Thus, the principle of symmetry breaking can be concisely phrased as follows:

Spurious minima break the symmetry of global minima.

The principle extends to more general target networks. When the isotropy of the target weight matrix V changes, so does the symmetry of spurious minima of the respective optimization problem. In Section A, we provide a series of experiments which empirically corroborates symmetry breaking for optimization problem (2).

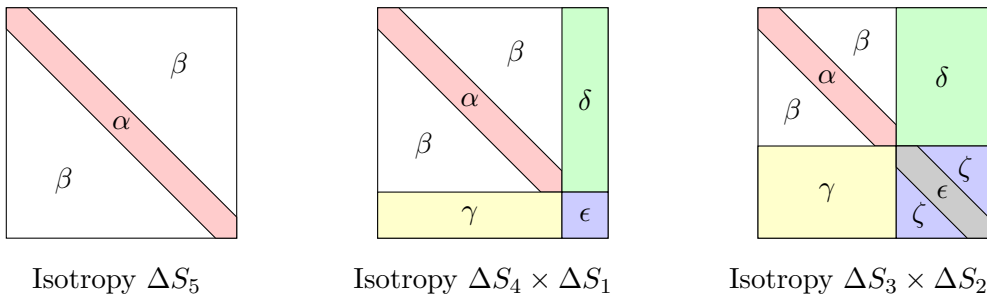


Figure 2: A schematic description of 5×5 matrices with isotropy ΔS_5 , $\Delta S_4 \times \Delta S_1$ and $\Delta S_3 \times \Delta S_2$, from left to right (borrowed from [2]). $\alpha, \beta, \gamma, \delta, \epsilon$ and ζ are assumed to be ‘sufficiently’ different.

The principle of symmetry breaking for ReLU networks was first studied in [2, 4], and was later extended to various tensor decomposition problems in [1]. Here, we analyze two-layer ReLU networks where *both* layers are trainable, an architecture which has received a great amount of attention in recent years [64, 16, 18, 38, 59, 10, 23]. We note in passing that, in its broader sense, the principle

of symmetry breaking has been observed many times in various scientific fields, e.g., Higgs-Landau theory, equivariant bifurcation theory and replica symmetry-breaking (see, e.g., [44, 29, 19, 14]). Two-layer ReLU networks seems to form a rather unexpected instance of this principle.

One intriguing quality of nonconvex landscapes in which the symmetry breaking principle applies is that local minima lie in fixed low-dimensional spaces (see Section 4). This phenomenon of a hidden low-dimensional structure has been observed in various learning problems in DL with real datasets [37, 30], and is believed by some researchers to be an important factor of learnability in nonconvex settings. In the context of this work, the hidden low-dimensionality of spurious minima turns out to be a key ingredient to our analytic study, as we now present.

2 Power series representation of families of spurious minima

Although the problem of fitting neural networks under the ST framework have been studied for more than 30 years, the symmetry breaking principle exhibited by optimization problem (2) seems to have gone largely unnoticed. Early studies adopted tools (at times, heuristic, e.g., [43, 42]) from statistical physics to analyze phase transitions and generalization errors [22, 55, 35, 60]. Later works focused on the dynamics of SGD and studied the evolution of the generalization error along the optimization process through a set of carefully-derived ODEs [17, 7, 50, 51, 49]. Following the empirical success of DL in the past decade, this line of work has recently drawn a renewed interest, e.g, [6, 27, 45, 28], which puts past analyses on rigorous grounds and addresses a broader class of architectures and activation functions. The analytic tools used in this long line of works operate in the *thermodynamic limit*—where the number of inputs is taken to infinity. Thus, the formal validity of the results to finite width networks is currently limited.

Other common approaches for analyzing problem (2) are based on: mean-field [41], optimal control [12], NTK [32] and compositional kernels [13]. These approaches offer, in essence, convex surrogates which apply in strict parameter regimes (including algorithmic parameters, such as learning rates). Similarly to the thermodynamic limit approach, the convex surrogates are obtained by limiting processes—this time by taking the number of hidden neurons to infinite. A growing number of works has severely limited, if not invalidated, the explanatory power of these approaches for network widths encountered in practice [63, 25].

In sharp contrast to the approaches discussed above, our technique directly addresses the associated highly nonconvex optimization landscape in the natural regime where the number of inputs and neurons is finite, and provides analytic, rather than heuristic, information. This is obtained by exploiting the presence of symmetry breaking phenomena whereby fractional power series representation for families of spurious minima are derived.

Below, we provide analytic expressions for families of minima of different isotropy (see Definition 3 and Figure 2), along with their respective objective value. For brevity, expressions are given to $O(d^{-3/2})$ -order. In the appendix, we list additional $O(d^{-5/2})$ -order terms which are required for computing the Hessian spectrum. The invariance properties of optimization problem (2) imply that additional families of minima can be obtained by permuting the rows and the columns of a given one. The number of new distinct minima generated using such transformations (i.e., multiplicity) depends on the very structure of the family of minima under consideration, and is stated in Theorem 1. Lastly, for any $\lambda > 0$ and $i \in [d]$, the value of the ReLU network (1) remains

fixed under $(\mathbf{w}_i, \alpha_i) \mapsto (\lambda \mathbf{w}_i, \alpha_i/\lambda)$. This degree-of-freedom is expressed by using the slack variables $\lambda_i > 0$, $i \in [d]$ below.

Theorem 1. *Optimization problem (2) with $k = d$, $V = I_d$ and $\beta = \mathbf{1}_d$ possesses the following families of minima for $d \geq 9$:*

1. *Two families of ΔS_d -minima of multiplicity $d!$ with $W(d) = \text{Diag}(\lambda_1, \dots, \lambda_d) A_d(a_1, a_2)$ and $\alpha(d) = (\lambda_1^{-1}, \dots, \lambda_d^{-1})$, where $\lambda_i > 0$,*

$$A_d(a_1, a_2) := \begin{pmatrix} a_1 & a_2 & \dots & & a_2 \\ a_2 & a_1 & a_2 & \dots & a_2 \\ & \vdots & & \ddots & \\ a_2 & \dots & & a_2 & a_1 \end{pmatrix} \in M(d, d),$$

$\text{Diag}(\cdot)$ maps a given vector to the diagonal entries of a diagonal matrix, and

- (a) $a_1 = 1$ and $a_2 = 0$ (a global minimizer), in which case

$$\mathcal{L}(W(d), \alpha(d)) = 0.$$

- (b) $a_1 = -1 + \frac{2}{d} + O(d^{-\frac{3}{2}})$, $a_2 = \frac{2}{d} + O(d^{-\frac{3}{2}})$, in which case

$$\mathcal{L}(W(d), \alpha(d)) = -\frac{1}{\pi} + \frac{1}{2} - \frac{4}{3\pi\sqrt{d}} + \frac{-\frac{1}{2} - \frac{2}{\pi^2} + \frac{3}{\pi}}{d} + O(d^{-\frac{3}{2}}). \quad (4)$$

2. *Two families of $\Delta(S_{d-1} \times S_1)$ -minima of multiplicity $d \cdot d!$ with*

$$W(d) = \text{Diag}(\lambda_1, \dots, \lambda_d) \left(\begin{array}{c|c} A_{d-1}(a_1, a_2) & a_3 \mathcal{I}_{d-1,1} \\ \hline a_4 \mathcal{I}_{1,d-1} & a_5 \end{array} \right),$$

and $\alpha(d) = (\lambda_1^{-1}, \dots, \lambda_d^{-1})$, where $\lambda_i > 0$ and

- (a) $a_1 = 1 + O(d^{-\frac{3}{2}})$, $a_2 = O(d^{-\frac{3}{2}})$, $a_3 = \frac{2}{d} + O(d^{-\frac{3}{2}})$, $a_4 = \frac{4}{\pi d} + O(d^{-\frac{3}{2}})$ and $a_5 = -1 + \frac{\frac{8}{\pi^2} + 2 + \frac{8}{\pi}}{d} + O(d^{-\frac{3}{2}})$, in which case

$$\mathcal{L}(W(d), \alpha(d)) = \frac{\frac{1}{2} - \frac{2}{\pi^2}}{d} + O(d^{-\frac{3}{2}}). \quad (5)$$

- (b) $a_1 = -1 + \frac{2}{d} + O(d^{-\frac{3}{2}})$, $a_2 = \frac{2}{d} + O(d^{-\frac{3}{2}})$, $a_3 = O(d^{-\frac{3}{2}})$, $a_4 = \frac{2 - \frac{4}{\pi}}{d} + O(d^{-\frac{3}{2}})$ and $a_5 = 1 + \frac{8(-1+\pi)}{\pi^2 d} + O(d^{-\frac{3}{2}})$, in which case

$$\mathcal{L}(W(d), \alpha(d)) = -\frac{1}{\pi} + \frac{1}{2} - \frac{4}{3\pi\sqrt{d}} + \frac{-1 - \frac{4}{\pi^2} + \frac{5}{\pi}}{d} + O(d^{-\frac{3}{2}}). \quad (6)$$

3. Two families of $\Delta(S_{d-2} \times S_2)$ -minima of multiplicity $d! \binom{d}{2}$ with

$$W(d) = \text{Diag}(\lambda_1, \dots, \lambda_d) \left(\begin{array}{c|c} A_{d-2}(a_1, a_2) & a_3 \mathcal{I}_{d-2,2} \\ \hline a_4 \mathcal{I}_{2,d-2} & A_2(a_5, a_6) \end{array} \right),$$

and $\alpha(d) = (\lambda_1^{-1}, \dots, \lambda_d^{-1})$, where $\lambda_i > 0$ and

$$(a) \quad a_1 = 1 + O\left(d^{-\frac{3}{2}}\right), \quad a_2 = 0 + O\left(d^{-\frac{3}{2}}\right), \quad a_3 = \frac{2}{d} + O\left(d^{-\frac{3}{2}}\right), \quad a_4 = \frac{4}{\pi d} + O\left(d^{-\frac{3}{2}}\right), \quad a_5 = -1 + \frac{\frac{8}{\pi^2} + 2 + \frac{8}{\pi}}{d} + O\left(d^{-\frac{3}{2}}\right) \text{ and } a_6 = \frac{2(-12\pi + 16 + \pi^3 + 4\pi^2)}{\pi^2 d(2 + \pi)} + O\left(d^{-\frac{3}{2}}\right), \text{ in which case}$$

$$\mathcal{L}(W(d), \alpha(d)) = \frac{-4 + \pi^2}{\pi^2 d} + O\left(d^{-\frac{3}{2}}\right). \quad (7)$$

$$(b) \quad a_1 = -1 + \frac{2}{d} + O\left(d^{-\frac{3}{2}}\right), \quad a_2 = \frac{2}{d} + O\left(d^{-\frac{3}{2}}\right), \quad a_3 = 0 + O\left(d^{-\frac{3}{2}}\right), \quad a_4 = \frac{2 - \frac{4}{\pi}}{d} + O\left(d^{-\frac{3}{2}}\right), \quad a_5 = 1 + \frac{8(-1 + \pi)}{\pi^2 d} + O\left(d^{-\frac{3}{2}}\right) \text{ and } a_6 = \frac{4(-\pi^2 - 8 + 6\pi)}{\pi^2 d(2 + \pi)} + O\left(d^{-\frac{3}{2}}\right), \text{ in which case}$$

$$\mathcal{L}(W(d), \alpha(d)) = -\frac{1}{\pi} + \frac{1}{2} - \frac{4}{3\pi\sqrt{d}} + \frac{-\frac{3}{2} - \frac{6}{\pi^2} + \frac{7}{\pi}}{d} + O\left(d^{-\frac{3}{2}}\right). \quad (8)$$

4. One family of $\Delta(S_{d-3} \times S_3)$ -minima of multiplicity $d! \binom{d}{3}$ with

$$W(d) = \text{Diag}(\lambda_1, \dots, \lambda_d) \left(\begin{array}{c|c} A_{d-3}(a_1, a_2) & a_3 \mathcal{I}_{d-3,3} \\ \hline a_4 \mathcal{I}_{3,d-3} & A_2(a_5, a_6) \end{array} \right),$$

and $\alpha(d) = (\lambda_1^{-1}, \dots, \lambda_d^{-1})$, where $\lambda_i > 0$ and $a_1 = 1 + O\left(d^{-\frac{3}{2}}\right)$, $a_2 = O\left(d^{-\frac{3}{2}}\right)$, $a_3 = \frac{2}{d} + O\left(d^{-\frac{3}{2}}\right)$, $a_4 = \frac{4}{\pi d} + O\left(d^{-\frac{3}{2}}\right)$, $a_5 = -1 + \frac{\frac{8}{\pi^2} + 2 + \frac{8}{\pi}}{d} + O\left(d^{-\frac{3}{2}}\right)$ and $a_6 = \frac{2(-12\pi + 16 + \pi^3 + 4\pi^2)}{\pi^2 d(2 + \pi)} + O\left(d^{-\frac{3}{2}}\right)$, in which case

$$\mathcal{L}(W(d), \alpha(d)) = \frac{\frac{3}{2} - \frac{6}{\pi^2}}{d} + O\left(d^{-\frac{3}{2}}\right). \quad (9)$$

The idea of the proof of [Theorem 1](#) is given in [Section 4.1](#), and the multiplicity computation, a simple application of the orbit-stabilizer theorem, in [Section B](#). We note that the same technique can be used for other choices of target networks, mutatis mutandis. The power series stated in [Theorem 1](#) also represent spurious minima for the under-parameterized $d > k$ -case. This is obtained by appropriately padding the entries of the weight matrices by zeros (see [[4](#), section 4.3] for details). The derivation of the respective Hessian spectrum is then an immediate application of [[3](#), section E.1] to the spectral analysis given in [Theorem 2](#) below (for the case where $d = k$). By contrast, studying the over-parameterized regime for which $d < k$ requires qualitatively different tools and is outside the scope of this work.

The analysis above reveals that not all local minima are alike: while the objective value of some minima decays like $\Theta(1/d)$, in other cases the objective value converges to the positive constant $\frac{1}{2} - \frac{1}{\pi}$. In particular, except for the global minima case [1a](#), all minima described above are spurious.

The difference between the two types of behavior seems to lie in the limiting values of the entries of $W(d)$; in the former, the diagonal mainly consists of ones, whereas in the latter mainly minus ones. This is consistent with the fact that all the teacher’s diagonal entries are ones.

For reasons which are yet to be understood, empirically, the bias induced by Xavier initialization [26] seems to favor the class of minima for which the objective value decays as $\Theta(1/d)$. This is not to say that under Xavier initialization the expected value upon convergence must decrease with d . The objective value decays to zero at different rates (see cases 2a, 3a, 4 above) and depends on the probability to converge to a given type of minima. (A possible proxy to the latter is the minima multiplicity stated in Theorem 1.)

3 Analytic study of the Hessian spectrum

Once a power series representation has been obtained, it is possible to analytically characterize various important properties of families of minima. Here, we use this representation to compute yet another fractional power series—this time, of the Hessian spectrum.

Theorem 2. *Assuming all the weights of the second layer of (1) are normalized to one, the (nonnegative) Hessian spectrum of the families of minima considered in Theorem 1 is*

<i>Eigenvalue</i>	<i>Multiplicity</i>
$O(d^{-1/2})$	d
$\frac{1}{4} - \frac{1}{2\pi} + O(d^{-1/2})$	$\frac{(d-1)(d-2)}{2}$
$\frac{1}{2} - \frac{1}{\pi} + O(d^{-1/2})$	$d - 1$
$\frac{1}{4} + O(d^{-1/2})$	$d - 1$
$\frac{1}{4} + \frac{1}{2\pi} + O(d^{-1/2})$	$\frac{d(d-3)}{2}$
$\frac{d}{4} + \frac{1}{2} + O(d^{-1/2})$	$d - 1$
$\frac{d}{4} + \frac{-4+\pi+\pi^2}{2\pi(-4+\pi)} + O(d^{-1/2})$	1
$\frac{d}{\pi} + \frac{-10\pi+8+\pi^2}{2\pi(-4+\pi)} + O(d^{-1/2})$	1.

The method we developed for computing the Hessian spectrum builds on [3], but differs in three crucial aspects. First, in our setting the second layer is trainable. The associated so-called *isotypic decomposition* (a set of ‘simple’ subspaces compatible with the action of row- and column-permutations formally introduced in Section D) must therefore cover the space of $d \times d$ weight matrices, as well as the d weights of the second layer. Secondly, rather than expressing the Hessian entries in terms of $d, W(d)$ and $\alpha(d)$ and then extracting fractional power series for eigenvalues, we directly express the eigenvalues in these terms. This considerably simplifies computations and facilitates the computation of eigenvalues to potentially any order. Thirdly, and perhaps most importantly, computing the Hessian to high accuracy reveals that for small values of d the families of minima presented in Theorem 1 are in fact saddles. Regarding d as a real number, we pinpoint the exact *fractional* dimension at which a given family of critical points turns from saddles into spurious minima (see also Figure 1). One is now led into the dual question: is there a mechanism by which spurious minima may be annihilated (that is, turn into saddles)? We have found that the process of the creation of minima can be reversed in the over-parameterized regime. This provides a

strong evidence for the benefits of increasing the number of student neurons from an optimization point of view—adding more neurons turns spurious minima into saddles makes, thus encouraging gradient-based methods to converge to minima of higher quality. A rigorous study of this process requires tools from the equivariant bifurcation theory, and is deferred to future work (cf. [5]).

Quite remarkably, although the families of minima presented in [Theorem 1](#) differ significantly, their Hessian spectra coincide to $O(d^{-1/2})$ -order. Another noticeable implication of [Theorem 2](#) is that the Hessian spectrum tends to be extremely skewed. Both phenomena, as well as their consequences for optimization-related aspects, are discussed below in detail.

Positively-skewed Hessian spectral density. Although first reported nearly 30 years ago [9], to our knowledge, this is the first time that this phenomenon of extremely skewed spectral density has been established *rigorously* for two trainable ReLU layers of arbitrarily large dimensionality. Early empirical studies of the Hessian spectrum [9] revealed that local minima tend to be extremely ill-conditioned. This intriguing observation was corroborated and further refined in a series of works [36, 53, 54] which studied how the spectrum evolves along the training process. It was noticed that, upon convergence, the spectral density decomposes into two parts: a bulk of eigenvalues concentrated near small positive constants, and a small set of positive outliers located away from zero.

Due to the high computational cost of an exact computation of the Hessian spectrum (cubic in the problem parameters k and d), this phenomenon of extremely skewed spectral densities has only been confirmed for small-scale networks. Other methods for extracting second-order information in large-scale problems roughly fall into two general categories. The first class of methods approximate the Hessian spectral density by employing various numerical estimation techniques, most notably stochastic Lanczos method (e.g., [24, 46]). These methods have provided various numerical evidences which indicate that a similar skewed spectrum phenomenon also occurs in full-scale modern neural networks. The second class of techniques builds on tools from random matrix theory. The latter approach yields an exact computation of the limiting spectral distribution (where the number of neurons is taken to infinity), assuming the inputs, as well as the model weights are drawn at random [47, 48, 39]. In contrast, our method gives an analytic description of the spectral density for any number of neurons (granted $d \geq 9$), and at critical points rather than randomly drawn weight matrices.

The flat minima conjecture and implicit bias. It has long been debated whether some notion of local curvature can be used to explain the remarkable generalization capabilities of modern neural networks [31, 34, 33, 61, 62, 11, 15]. One intriguing hypothesis argues that minima with wider basins of attraction tend to generalize better. The suggested intuitive explanation is that flat minima promote statistical and numerical stability; together with low empirical loss, these ingredients are widely used to achieve good generalization, cf. [56]. However, the analysis presented in [Theorem 2](#) shows that the spectra of global minima and spurious minima agree to $O(d^{-1/2})$ -order. Consequently, in our setting, local second-order curvature *cannot* be used to separate global from spurious minima. This rules out any notions of ‘flatness’ which rely exclusively on the Hessian spectrum. Of course, other metrics of a ‘wideness of basins’ may be applied.

4 A symmetry-based analytic framework

In the sequel, we present the main ingredients of the symmetry-based technique developed in this work. The technique builds on, and significantly extends various components from [3, 2, 4]. To ease exposition, we illustrate with reference to the case where $k = d$ and the second layer is kept fixed with entries equal ones. We denote the resulting nonconvex function by $f(W) := \mathcal{L}(W, \mathbf{1})$.

4.1 Power series representation of minima

The first step in deriving a power series representation is to restrict the nonconvex function under consideration to *fixed point subspaces* (see [20] for a more complete account) that consists of weight matrices which remain fixed under row- and column-permutations in a certain subgroup of $S_d \times S_d$. For concreteness, consider the space of all matrices which are invariant to permutations in ΔS_d , i.e.,

$$\mathcal{W}_d := \{W \in M(d, d) \mid W = P_\pi W P_\pi^\top \text{ for all } (\pi, \pi) \in \Delta S_d\}. \quad (10)$$

It is easy to verify that \mathcal{W}_d is in fact a 2-dimensional subspace of the form $\mathcal{W}_d = \{(a_1, a_2) \mid a_1 I_d + a_2(\mathbf{1}_d \mathbf{1}_d^\top - I)\}$, and that if $W \in \mathcal{W}_d$, then also $\nabla f(W) \in \mathcal{W}_d$ (see [2, Proposition 3]). Thus, one may regard f as a function from \mathbb{R}^2 to \mathbb{R}^2 . Next, we make the dependence of f on d explicit by defining $F : \mathbb{R}^3 \rightarrow \mathbb{R}^2 : (a_1, a_2, d) \mapsto \nabla f(a_1 I_d + a_2(\mathbf{1}_d \mathbf{1}_d^\top - I_d))$. Note that although d is a natural number, the following explicit expressions of the entries of $F(a_1, a_2, d)$ allows us to regard d as a real variable:

$$\left(\begin{array}{c} \frac{a_1 d}{2} - \frac{a_1 d \sin(\beta_{(1)}^{(1)})}{2\pi\nu_{(1)}} + \frac{a_1(d^2-d) \sin(\alpha_{(1)}^{(2)})}{2\pi} - \frac{a_1(d^2-d) \sin(\beta_{(1)}^{(2)})}{2\pi\nu_{(1)}} - \frac{a_2 \alpha_{(1)}^{(2)}(d^2-d)}{2\pi} + \frac{a_2(d^2-d)}{2} + \frac{\beta_{(1)}^{(1)} d}{2\pi} - \frac{d}{2} \\ -\frac{a_1 \alpha_{(1)}^{(2)}(d^2-d)}{2\pi} + \frac{a_1(d^2-d)}{2} - \frac{a_2 \alpha_{(1)}^{(2)}(d^3-3d^2+2d)}{2\pi} + \frac{a_2(d^3-2d^2+d) \sin(\alpha_{(1)}^{(2)})}{2\pi} + \frac{a_2(d^3-2d^2+d)}{2} - \frac{a_2(d^2-d) \sin(\beta_{(1)}^{(1)})}{2\pi\nu_{(1)}} - \frac{a_2(d^3-2d^2+d) \sin(\beta_{(1)}^{(2)})}{2\pi\nu_{(1)}} + \frac{\beta_{(1)}^{(2)}(d^2-d)}{2\pi} - \frac{d^2}{2} + \frac{d}{2} \end{array} \right)$$

where, here and below, $\alpha_{(i)}^{(j)}$ (resp. $\beta_{(i)}^{(j)}$) denotes the angles between the i th row of W and the j th of W (resp. V). Using the implicit function theorem one can establish the existence (as well as the uniqueness) of a path of critical points $(a_1(d), a_2(d))$. This gives a formal meaning for examining a given family of minima at a *fractional* dimensionality. The necessary formalities are covered in [4].

We are left with the following two main issues. First, the implicit function theorem does not yield an explicit form of $a_1(d)$ and $a_2(d)$. This issue is addressed by using a *real analytic* version of the implicit function theorem, and then computing the coefficients of the power series of $a_1(d)$ and $a_2(d)$ to the desired order. Secondly, the implicit function theorem requires initial values for a_1 and a_2 which solve $F(a_1, a_2, d) = 0$. To handle this issue, we form power series in $1/d$ and, loosely speaking, develop them at $d = \infty$. The advantage of this nonstandard manipulation is that the limiting entries of $W(d)$ have a very simple form, which are then used as the initial values required for invoking the implicit function theorem. In fact, due to the dependence of ∇f on the angles between rows of W and V , the power series of $a_1(d)$ and $a_2(d)$ are expressed in terms of $1/\sqrt{d}$. [Theorem 1](#) is established by following the recipe described here for various families of critical points of different isotropy. The gradient expressions involved in the process are lengthy and are therefore relegated to [Section E](#).

4.2 Computing the Hessian spectrum

Our next goal is to derive an analytic characterization of the Hessian spectrum. The invariance properties of \mathcal{L} imply that although the dimension of the Hessian, $k(d+1) \times k(d+1)$, depends on

k and d , the number of distinct eigenvalues remains fixed. This is an immediate consequence of the corresponding isotypic decomposition (see [Section D](#)). A formal introduction of the isotypic decomposition requires some familiarity with group actions, and is therefore deferred to [Section D.2](#). Here, we shall focus on one particularly simple case.

The isotypic decomposition associated with ΔS_d , the isotropy of I_d , implies that for any d ,

$$\overline{\mathfrak{Y}}_d := \text{vec} \begin{pmatrix} \begin{bmatrix} 0 & d-3 & 3-d & \cdots & 0 & 0 & 0 \\ d-3 & 0 & 0 & \cdots & -1 & -1 & -1 \\ 3-d & 0 & 0 & \cdots & 1 & 1 & 1 \\ 0 & -1 & 1 & \cdots & 0 & 0 & 0 \\ \cdots & \cdots & \cdots & \cdots & \cdots & \cdots & \cdots \\ 0 & -1 & 1 & \cdots & 0 & 0 & 0 \\ 0 & -1 & 1 & \cdots & 0 & 0 & 0 \end{bmatrix} \end{pmatrix},$$

is an eigenvector of $\nabla^2 f(I_d)$, where vec denotes the linear transformation which stacks the rows of a given matrix on top of one another as a column vector. Thus, the eigenvalue corresponding to $\overline{\mathfrak{Y}}_d$ equals $(\nabla^2 f(I_d)\overline{\mathfrak{Y}}_d)_2/(d-3)$, which takes the following explicit form

$$\frac{a_1^2}{2\pi\nu_{(1)}^2\nu_{(1)}^{(2)}} + \frac{a_1^2 \sin(\alpha_{(1)}^{(2)})}{2\pi\nu_{(1)}^2(\nu_{(1)}^{(2)})^2} - \frac{a_1 a_2}{\pi\nu_{(1)}^2\nu_{(1)}^{(2)}} - \frac{a_1 a_2 \sin(\alpha_{(1)}^{(2)})}{\pi\nu_{(1)}^2(\nu_{(1)}^{(2)})^2} + \frac{a_2^2}{2\pi\nu_{(1)}^2\nu_{(1)}^{(2)}} + \frac{a_2^2 \sin(\alpha_{(1)}^{(2)})}{2\pi\nu_{(1)}^2(\nu_{(1)}^{(2)})^2} + \frac{\alpha_{(1)}^{(2)}}{2\pi} + \frac{(d-1) \sin(\alpha_{(1)}^{(2)})}{2\pi} - \frac{(d-1) \sin(\beta_{(1)}^{(2)})}{2\pi\nu_{(1)}} - \frac{\sin(\beta_{(1)}^{(1)})}{2\pi\nu_{(1)}} - \frac{\sin(\beta_{(1)}^{(2)})}{2\pi(\mu_{(1)}^{(2)})^2\nu_{(1)}},$$

where $\nu_{(i)}$ denotes the norm of the i th row of W , and $\nu_{(i)}^{(j)}$ (resp. $\mu_{(i)}^{(j)}$) denotes $\sin \arccos(\alpha_{(i)}^{(j)})$ (resp. $\sin \arccos(\beta_{(i)}^{(j)})$). To complete the derivation of the eigenvalue $\overline{\mathfrak{Y}}_d$ for families of isotropy ΔS_d , e.g., cases 1(a) and 1(b) in [Theorem 1](#), one plugs-in the power series representation of $a_1(d)$ and $a_2(d)$ into the expression above, and forms a new power series to get an estimate for $\overline{\mathfrak{Y}}_d$. The same procedure is used for all families of minima presented in [Theorem 1](#), and is described in detail in [Section 4.2](#).

5 Conclusion

When present, the principle of symmetry breaking forms a powerful tool of dramatically reducing the complexity of nonconvex problems in a nonlinear way. This yields unprecedented analytic information for ReLU networks with a finite number of inputs and neurons, rather than limiting models of varying qualities. At this stage of the theory, the extent to which the symmetry breaking principle applies is far from being clear. However, it does seem to hold in a broader class of fundamental nonconvex problems, e.g., [\[1\]](#).

We further remark that the families of spurious minima studied in this paper are illustrative examples in which an exceptional proximity to the objective value and the hessian spectrum is allowed. One intriguing finding is that spurious and global minima are locally identical to $O(d^{-1/2})$ -order. Considering the fact that the multiplicity local minima for $k = d$ is essentially exponential in d , it is rather unlikely for SGD to be able to escape spurious minima when d grows (see [\[52, Table 1\]](#)). Why is it then that SGD is generally able to find good minima for optimization problems associated with fitting ReLU neural networks? Preliminary experiments we conducted indicate that *continuously* increasing k and leaving d fixed turns families of spurious minima turn into saddles (the objective value seems to remain constant). We believe that this observation is instrumental

in explaining the empirical success of SGD for DL problem. A thorough study of this phenomenon requires tools from equivariant bifurcation theory and is postponed to future work.

References

- [1] Yossi Arjevani, Joan Bruna, Michael Field, Joe Kileel, Matthew Trager, and Francis Williams. Symmetry breaking in symmetric tensor decomposition. *arXiv preprint arXiv:2103.06234*, 2021.
- [2] Yossi Arjevani and Michael Field. On the principle of least symmetry breaking in shallow relu models. *arXiv preprint arXiv:1912.11939*, 2019.
- [3] Yossi Arjevani and Michael Field. Analytic characterization of the hessian in shallow relu models: A tale of symmetry. *arXiv preprint arXiv:2008.01805*, 2020.
- [4] Yossi Arjevani and Michael Field. Symmetry & critical points for a model shallow neural network. *CoRR*, abs/2003.10576, 2020.
- [5] Yossi Arjevani and Michael Field. Equivariant bifurcation, quadratic equivariants, and symmetry breaking for the standard representation of s_n . *arXiv preprint arXiv:2107.02422*, 2021.
- [6] Benjamin Aubin, Antoine Maillard, Jean Barbier, Florent Krzakala, Nicolas Macris, and Lenka Zdeborová. The committee machine: Computational to statistical gaps in learning a two-layers neural network. *Journal of Statistical Mechanics: Theory and Experiment*, 2019(12):124023, 2019.
- [7] Michael Biehl and Holm Schwarze. Learning by on-line gradient descent. *Journal of Physics A: Mathematical and general*, 28(3):643, 1995.
- [8] Avrim L Blum and Ronald L Rivest. Training a 3-node neural network is np-complete. *Neural Networks*, 5(1):117–127, 1992.
- [9] Léon Bottou. Stochastic gradient learning in neural networks. *Proceedings of Neuro-Nimes*, 91(8):12, 1991.
- [10] Alon Brutzkus and Amir Globerson. Globally optimal gradient descent for a convnet with gaussian inputs. In *Proceedings of the 34th International Conference on Machine Learning-Volume 70*, pages 605–614. JMLR. org, 2017.
- [11] Pratik Chaudhari, Anna Choromanska, Stefano Soatto, Yann LeCun, Carlo Baldassi, Christian Borgs, Jennifer Chayes, Levent Sagun, and Riccardo Zecchina. Entropy-sgd: Biasing gradient descent into wide valleys. *Journal of Statistical Mechanics: Theory and Experiment*, 2019(12):124018, 2019.
- [12] Lenaïc Chizat and Francis Bach. On the global convergence of gradient descent for over-parameterized models using optimal transport. *arXiv preprint arXiv:1805.09545*, 2018.
- [13] Amit Daniely, Roy Frostig, and Yoram Singer. Toward deeper understanding of neural networks: The power of initialization and a dual view on expressivity. *arXiv preprint arXiv:1602.05897*, 2016.

- [14] Jian Ding, Allan Sly, and Nike Sun. Proof of the satisfiability conjecture for large k . In *Proceedings of the Forty-Seventh Annual ACM on Symposium on Theory of Computing, STOC 2015, Portland, OR, USA, June 14-17, 2015*, pages 59–68, 2015.
- [15] Laurent Dinh, Razvan Pascanu, Samy Bengio, and Yoshua Bengio. Sharp minima can generalize for deep nets. In *Proceedings of the 34th International Conference on Machine Learning-Volume 70*, pages 1019–1028. JMLR. org, 2017.
- [16] Simon S. Du, Jason D. Lee, Yuandong Tian, Aarti Singh, and Barnabás Póczos. Gradient descent learns one-hidden-layer CNN: don’t be afraid of spurious local minima. In *Proceedings of the 35th International Conference on Machine Learning, ICML 2018, Stockholmsmässan, Stockholm, Sweden, July 10-15, 2018*, pages 1338–1347, 2018.
- [17] Andreas Engel and Christian Van den Broeck. *Statistical mechanics of learning*. Cambridge University Press, 2001.
- [18] Soheil Feizi, Hamid Javadi, Jesse Zhang, and David Tse. Porcupine neural networks:(almost) all local optima are global. *arXiv preprint arXiv:1710.02196*, 2017.
- [19] M. J. Field and R. W. Richardson. Symmetry breaking and the maximal isotropy subgroup conjecture for reflection groups. *Archive for Rational Mechanics and Analysis*, 105(1):61–94, Mar 1989.
- [20] Michael J. Field. *Dynamics and symmetry*, volume 3 of *ICP Advanced Texts in Mathematics*. Imperial College Press, London, 2007.
- [21] William Fulton and Joe Harris. Representation theory, volume 129 of. *Graduate Texts in Mathematics*, 1991.
- [22] Elizabeth Gardner and Bernard Derrida. Three unfinished works on the optimal storage capacity of networks. *Journal of Physics A: Mathematical and General*, 22(12):1983, 1989.
- [23] Rong Ge, Jason D. Lee, and Tengyu Ma. Learning one-hidden-layer neural networks with landscape design. In *6th International Conference on Learning Representations, ICLR 2018, Vancouver, BC, Canada, April 30 - May 3, 2018, Conference Track Proceedings*, 2018.
- [24] Behrooz Ghorbani, Shankar Krishnan, and Ying Xiao. An investigation into neural net optimization via hessian eigenvalue density. In Kamalika Chaudhuri and Ruslan Salakhutdinov, editors, *Proceedings of the 36th International Conference on Machine Learning, ICML 2019, 9-15 June 2019, Long Beach, California, USA*, volume 97 of *Proceedings of Machine Learning Research*, pages 2232–2241. PMLR, 2019.
- [25] Behrooz Ghorbani, Song Mei, Theodor Misiakiewicz, and Andrea Montanari. When do neural networks outperform kernel methods? *arXiv preprint arXiv:2006.13409*, 2020.
- [26] Xavier Glorot and Yoshua Bengio. Understanding the difficulty of training deep feedforward neural networks. In *Proceedings of the thirteenth international conference on artificial intelligence and statistics*, pages 249–256, 2010.
- [27] Sebastian Goldt, Madhu S Advani, Andrew M Saxe, Florent Krzakala, and Lenka Zdeborová. Dynamics of stochastic gradient descent for two-layer neural networks in the teacher-student setup. *arXiv preprint arXiv:1906.08632*, 2019.

- [28] Sebastian Goldt, Madhu S Advani, Andrew M Saxe, Florent Krzakala, and Lenka Zdeborová. Generalisation dynamics of online learning in over-parameterised neural networks. *arXiv preprint arXiv:1901.09085*, 2019.
- [29] Martin Golubitsky. The benard problem, symmetry and the lattice of isotropy subgroups. *Bifurcation Theory, Mechanics and Physics. CP Boner et al., eds.(Reidel, Dordrecht, 1983)*, pages 225–256, 1983.
- [30] Guy Gur-Ari, Daniel A Roberts, and Ethan Dyer. Gradient descent happens in a tiny subspace. *arXiv preprint arXiv:1812.04754*, 2018.
- [31] Sepp Hochreiter and Jürgen Schmidhuber. Flat minima. *Neural Computation*, 9(1):1–42, 1997.
- [32] Arthur Jacot, Franck Gabriel, and Clément Hongler. Neural tangent kernel: Convergence and generalization in neural networks. *arXiv preprint arXiv:1806.07572*, 2018.
- [33] Stanislaw Jastrzebski, Zachary Kenton, Devansh Arpit, Nicolas Ballas, Asja Fischer, Yoshua Bengio, and Amos Storkey. Three factors influencing minima in sgd. *arXiv preprint arXiv:1711.04623*, 2017.
- [34] Nitish Shirish Keskar, Dheevatsa Mudigere, Jorge Nocedal, Mikhail Smelyanskiy, and Ping Tak Peter Tang. On large-batch training for deep learning: Generalization gap and sharp minima. *arXiv preprint arXiv:1609.04836*, 2016.
- [35] W Kinzel and Pal Rujan. Improving a network generalization ability by selecting examples. *EPL (Europhysics Letters)*, 13(5):473, 1990.
- [36] Yann A LeCun, Léon Bottou, Genevieve B Orr, and Klaus-Robert Müller. Efficient backprop. In *Neural networks: Tricks of the trade*, pages 9–48. Springer, 2012.
- [37] Chunyuan Li, Heerad Farkhoor, Rosanne Liu, and Jason Yosinski. Measuring the intrinsic dimension of objective landscapes. *arXiv preprint arXiv:1804.08838*, 2018.
- [38] Yuanzhi Li and Yang Yuan. Convergence analysis of two-layer neural networks with relu activation. In *Advances in Neural Information Processing Systems*, pages 597–607, 2017.
- [39] Cosme Louart, Zhenyu Liao, Romain Couillet, et al. A random matrix approach to neural networks. *The Annals of Applied Probability*, 28(2):1190–1248, 2018.
- [40] Stefano Sarao Mannelli, Eric Vanden-Eijnden, and Lenka Zdeborová. Optimization and generalization of shallow neural networks with quadratic activation functions. *arXiv preprint arXiv:2006.15459*, 2020.
- [41] Song Mei, Andrea Montanari, and Phan-Minh Nguyen. A mean field view of the landscape of two-layer neural networks. *Proceedings of the National Academy of Sciences*, 115(33):E7665–E7671, 2018.
- [42] Marc Mezard and Andrea Montanari. *Information, physics, and computation*. Oxford University Press, 2009.
- [43] Marc Mézard, Giorgio Parisi, and Miguel Angel Virasoro. *Spin glass theory and beyond: An Introduction to the Replica Method and Its Applications*, volume 9. World Scientific Publishing Company, 1987.

- [44] L Michel. Minima of higgs-landau polynomials. Technical report, 1979.
- [45] Elisa Oostwal, Michiel Straat, and Michael Biehl. Hidden unit specialization in layered neural networks: Relu vs. sigmoidal activation. *Physica A: Statistical Mechanics and its Applications*, 564:125517, 2021.
- [46] Vardan Papyan. The full spectrum of deepnet hessians at scale: Dynamics with sgd training and sample size. *arXiv preprint arXiv:1811.07062*, 2018.
- [47] Jeffrey Pennington and Pratik Worah. Nonlinear random matrix theory for deep learning. In *Advances in Neural Information Processing Systems*, pages 2637–2646, 2017.
- [48] Jeffrey Pennington and Pratik Worah. The spectrum of the fisher information matrix of a single-hidden-layer neural network. In *Advances in Neural Information Processing Systems*, pages 5410–5419, 2018.
- [49] Peter Riegler and Michael Biehl. On-line backpropagation in two-layered neural networks. *Journal of Physics A: Mathematical and General*, 28(20):L507, 1995.
- [50] David Saad and Sara A Solla. Exact solution for on-line learning in multilayer neural networks. *Physical Review Letters*, 74(21):4337, 1995.
- [51] David Saad and Sara A Solla. On-line learning in soft committee machines. *Physical Review E*, 52(4):4225, 1995.
- [52] Itay Safran and Ohad Shamir. Spurious local minima are common in two-layer relu neural networks. In *Proceedings of the 35th International Conference on Machine Learning, ICML 2018, Stockholmsmässan, Stockholm, Sweden, July 10-15, 2018*, pages 4430–4438, 2018.
- [53] Levent Sagun, Leon Bottou, and Yann LeCun. Eigenvalues of the hessian in deep learning: Singularity and beyond. *arXiv preprint arXiv:1611.07476*, 2016.
- [54] Levent Sagun, Utku Evci, V Ugur Guney, Yann Dauphin, and Leon Bottou. Empirical analysis of the hessian of over-parametrized neural networks. *arXiv preprint arXiv:1706.04454*, 2017.
- [55] Hyunjune Sebastian Seung, Haim Sompolinsky, and Naftali Tishby. Statistical mechanics of learning from examples. *Physical review A*, 45(8):6056, 1992.
- [56] Shai Shalev-Shwartz, Ohad Shamir, Nathan Srebro, and Karthik Sridharan. Learnability, stability and uniform convergence. *Journal of Machine Learning Research*, 11(Oct):2635–2670, 2010.
- [57] Ohad Shamir. Distribution-specific hardness of learning neural networks. *The Journal of Machine Learning Research*, 19(1):1135–1163, 2018.
- [58] Charles Benedict Thomas. *Representations of finite and Lie groups*. World Scientific, 2004.
- [59] Yuandong Tian. An analytical formula of population gradient for two-layered relu network and its applications in convergence and critical point analysis. In *Proceedings of the 34th International Conference on Machine Learning-Volume 70*, pages 3404–3413. JMLR. org, 2017.
- [60] Timothy LH Watkin, Albrecht Rau, and Michael Biehl. The statistical mechanics of learning a rule. *Reviews of Modern Physics*, 65(2):499, 1993.

- [61] Lei Wu, Zhanxing Zhu, et al. Towards understanding generalization of deep learning: Perspective of loss landscapes. *arXiv preprint arXiv:1706.10239*, 2017.
- [62] Zhewei Yao, Amir Gholami, Qi Lei, Kurt Keutzer, and Michael W Mahoney. Hessian-based analysis of large batch training and robustness to adversaries. In *Advances in Neural Information Processing Systems*, pages 4949–4959, 2018.
- [63] Gilad Yehudai and Ohad Shamir. On the power and limitations of random features for understanding neural networks. *arXiv preprint arXiv:1904.00687*, 2019.
- [64] Qiuyi Zhang, Rina Panigrahy, Sushant Sachdeva, and Ali Rahimi. Electron-proton dynamics in deep learning. *arXiv preprint arXiv:1702.00458*, pages 1–31, 2017.

A Symmetry breaking principle

A.1 $S_k \times S_d$ -invariance properties of (2)

We show that \mathcal{L} is $S_k \times S_d$ -invariant in its first parameter. The proof is a straightforward adaption of [2, Section 4.1]. First, we make the dependence of \mathcal{L} on the target weight $d \times d$ -matrix V explicit:

$$\bar{\mathcal{L}}(W, \alpha; V, \beta) := \frac{1}{2} \mathbb{E}_{\mathbf{x} \sim \mathcal{N}(\mathbf{0}, I_d)} \left[\left(\sum_{i=1}^k \alpha_i \varphi(\langle \mathbf{w}_i, \mathbf{x} \rangle) - \sum_{i=1}^d \beta_i \varphi(\langle \mathbf{v}_i, \mathbf{x} \rangle) \right)^2 \right], \quad (11)$$

Next, observe that for any $\pi \in S_k, \rho \in S_d$ and $U \in O(d)$, the group of all $d \times d$ -orthogonal matrices, we have

$$\bar{\mathcal{L}}(W, \alpha; V, \beta) = \bar{\mathcal{L}}(P_\pi W, \alpha; V, \beta) = \bar{\mathcal{L}}(W, \alpha; P_\rho V, \beta), \quad (12)$$

$$\bar{\mathcal{L}}(W, \alpha; V, \beta) = \bar{\mathcal{L}}(WU, \alpha; VU, \beta), \quad (13)$$

where the last equality follows by the $O(d)$ -invariance of the standard multivariate Gaussian distribution. Therefore, for any $\rho \in S_d$ and $U \in O(d)$ such that $V = P_\rho VU^\top$ and any $\pi \in S_k$, we have

$$\begin{aligned} \bar{\mathcal{L}}(W, \alpha, V, \beta) &= \bar{\mathcal{L}}(W, \alpha, P_\rho VU^\top, \beta) \stackrel{(12)}{=} \bar{\mathcal{L}}(W, \alpha, VU^\top, \beta) \stackrel{(13)}{=} \bar{\mathcal{L}}(WU, \alpha, VU^\top U, \beta) \\ &= \bar{\mathcal{L}}(WU, \alpha, V, \beta) \stackrel{(12)}{=} \bar{\mathcal{L}}(P_\pi WU, \alpha, V, \beta). \end{aligned}$$

In particular, for $V = I_d$, we have $V = P_\pi V P_\pi^\top$ for any $\pi \in S_d$, thus $\mathcal{L}(W, \alpha) = \bar{\mathcal{L}}(W, \alpha, I_d, \beta)$ is $S_k \times S_d$ -invariant w.r.t. W . Note that here we do not exploit the rotational invariance of the standard Gaussian distribution, but rather its invariance to permutations. Hence, the same $S_k \times S_d$ -invariance holds for any product distribution if $V = I_d$. Indeed, critical points admit maximal isotropy types also when the input distribution is $\mathcal{D} = \mathcal{U}([-1, 1]^d)$ (but not when $\mathcal{D} = \mathcal{U}([0, 2]^d)$).

A.2 Examples of minima for Problem (2)

We display several examples for optimization problem (2) with $k = d = 10$ obtained by running SGD until the gradient norm is driven below $1e-8$.

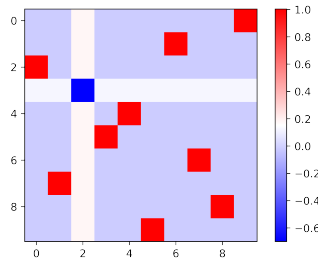


Figure 3: A spurious minimum of isotropy (conjugated to) $\Delta(S_{d-1} \times S_1)$ of (2) with $k = d = 10$. The objective value is ≈ 0.018 .

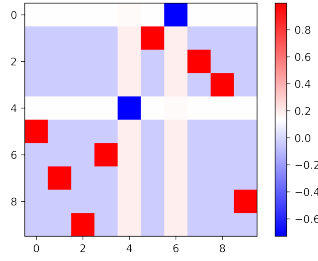


Figure 4: A spurious minimum of isotropy (conjugated to) $\Delta(S_{d-2} \times S_2)$ of (2) with $k = d = 10$. The objective value is ≈ 0.035 .

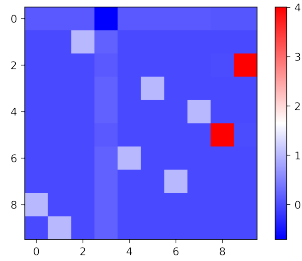


Figure 5: A spurious minimum of (2) with $k = d = 10$, where $V = \text{Diag}(1, \dots, 1, 2, 2)$ and $\beta = (1, \dots, 1, 2, 2)$. The symmetry of the minimum adapt to that of the global minimizer V .

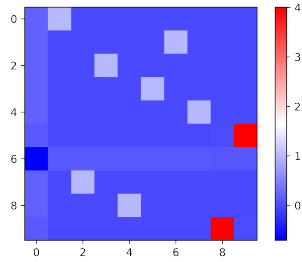


Figure 6: A spurious minimum of (2) with $k = d = 10$, where the $V = \text{Diag}(1, \dots, 1, 2, 2)$ and $\beta = (1, \dots, 1, 2, 2)$. The symmetry of the minimum adapt to that of the global minimizer V .

B Counting multiplicity of families of minima

The computation of the multiplicity of minima is based on the orbit-stabilizer theorem. Instantiating this theorem to the natural action of $S_k \times S_d$ (i.e., row- and column- permutation. See Section D.1

below for a formal introduction of group action) yields

$$\text{Multiplicity}(W) = \frac{|S_k \times S_d|}{|\text{Iso}(W)|}.$$

Observing that $|S_k \times S_d| = d! k!$, $|\Delta S_d| = d!$, $|\Delta(S_{d-1} \times S_1)| = (d-1)!$, $|\Delta(S_{d-2} \times S_2)| = (d-2)! 2!$ and $|\Delta(S_{d-3} \times S_3)| = (d-3)! 3!$ gives the multiplicities stated in [Theorem 1](#).

C Gradient expressions

In the sequel, we provide explicit expressions for $\nabla \mathcal{L}$ (defined in [\(2\)](#)) restricted the fixed point spaces $\mathcal{W}_{d-1}, \mathcal{W}_{d-2}, \mathcal{W}_{d-3}$, which naturally extend [Definition 10](#) as follows

$$\mathcal{W}_p := \{W \in M(d, d) \mid W = P_\pi W P_\pi^\top \text{ for all } (\pi, \pi) \in \Delta(S_{d-p} \times S_p)\}.$$

The gradient expressions corresponding to \mathcal{W}_d are given in the body of the paper in [Section 4.1](#).

In all expressions below:

- $\alpha_{(i)}^{(j)}$ (resp. $\beta_{(i)}^{(j)}$) denotes the angles between the i th row of W and the j th of W (resp. V , the target weight matrix).
- $\nu_{(i)}$ (resp. $\mu_{(i)}$) denotes the norm of the i th row of W (resp. V).
- $\nu_{(i)}^{(j)}$ (resp. $\mu_{(i)}^{(j)}$) denotes $\sin \arccos(\alpha_{(i)}^{(j)})$ (resp. $\sin \arccos(\beta_{(i)}^{(j)})$).

In [Section F](#), we list the coefficients of the families of minima considered in [Theorem 1](#) to $O(d^{-5/2})$ -order.

C.1 Gradient expressions for \mathcal{W}_1

The space \mathcal{W}_1 is five-dimensional. A weight matrix for $d = 8$ can be parameterized as follows

$$\begin{bmatrix} a_1 & a_2 & a_2 & a_2 & a_2 & a_2 & a_2 & a_3 \\ a_2 & a_1 & a_2 & a_2 & a_2 & a_2 & a_2 & a_3 \\ a_2 & a_2 & a_1 & a_2 & a_2 & a_2 & a_2 & a_3 \\ a_2 & a_2 & a_2 & a_1 & a_2 & a_2 & a_2 & a_3 \\ a_2 & a_2 & a_2 & a_2 & a_1 & a_2 & a_2 & a_3 \\ a_2 & a_2 & a_2 & a_2 & a_2 & a_1 & a_2 & a_3 \\ a_2 & a_2 & a_2 & a_2 & a_2 & a_2 & a_1 & a_3 \\ a_4 & a_4 & a_4 & a_4 & a_4 & a_4 & a_4 & a_5 \end{bmatrix}.$$

The gradient entries, denoted by g_1, g_2, g_3, g_4 and g_5 , are:

$$\begin{aligned}
g_1 &= \frac{a_1(d-1)}{2} + \frac{a_1(d^2-3d+2)\sin(\alpha_{(1)}^{(2)})}{2\pi} + \frac{a_1\nu_{(d)}(d-1)\sin(\alpha_{(1)}^{(d)})}{2\pi\nu_{(1)}} - \frac{a_1(d-1)\sin(\beta_{(1)}^{(1)})}{2\pi\nu_{(1)}} \\
&\quad - \frac{a_1(d-1)\sin(\beta_{(1)}^{(d)})}{2\pi\nu_{(1)}} - \frac{a_1(d^2-3d+2)\sin(\beta_{(1)}^{(2)})}{2\pi\nu_{(1)}} - \frac{a_2\alpha_{(1)}^{(2)}(d^2-3d+2)}{2\pi} \\
&\quad + \frac{a_2(d^2-3d+2)}{2} - \frac{a_4\alpha_{(1)}^{(d)}(d-1)}{2\pi} + \frac{a_4(d-1)}{2} + \frac{\beta_{(1)}^{(1)}(d-1)}{2\pi} - \frac{d}{2} + \frac{1}{2}, \\
g_2 &= -\frac{a_1\alpha_{(1)}^{(2)}(d^2-3d+2)}{2\pi} + \frac{a_1(d^2-3d+2)}{2} - \frac{a_2\alpha_{(1)}^{(2)}(d^3-6d^2+11d-6)}{2\pi} \\
&\quad + \frac{a_2(d^3-5d^2+8d-4)\sin(\alpha_{(1)}^{(2)})}{2\pi} + \frac{a_2(d^3-5d^2+8d-4)}{2} + \frac{a_2\nu_{(d)}(d^2-3d+2)\sin(\alpha_{(1)}^{(d)})}{2\pi\nu_{(1)}} \\
&\quad - \frac{a_2(d^2-3d+2)\sin(\beta_{(1)}^{(1)})}{2\pi\nu_{(1)}} - \frac{a_2(d^2-3d+2)\sin(\beta_{(1)}^{(d)})}{2\pi\nu_{(1)}} - \frac{a_2(d^3-5d^2+8d-4)\sin(\beta_{(1)}^{(2)})}{2\pi\nu_{(1)}} \\
&\quad - \frac{a_4\alpha_{(1)}^{(d)}(d^2-3d+2)}{2\pi} + \frac{a_4(d^2-3d+2)}{2} + \frac{\beta_{(1)}^{(2)}(d^2-3d+2)}{2\pi} - \frac{d^2}{2} + \frac{3d}{2} - 1, \\
g_3 &= -\frac{a_3\alpha_{(1)}^{(2)}(d^2-3d+2)}{2\pi} + \frac{a_3(d^2-3d+2)\sin(\alpha_{(1)}^{(2)})}{2\pi} + \frac{a_3(d^2-2d+1)}{2} \\
&\quad + \frac{a_3\nu_{(d)}(d-1)\sin(\alpha_{(1)}^{(d)})}{2\pi\nu_{(1)}} - \frac{a_3(d-1)\sin(\beta_{(1)}^{(1)})}{2\pi\nu_{(1)}} - \frac{a_3(d-1)\sin(\beta_{(1)}^{(d)})}{2\pi\nu_{(1)}} \\
&\quad - \frac{a_3(d^2-3d+2)\sin(\beta_{(1)}^{(2)})}{2\pi\nu_{(1)}} - \frac{a_5\alpha_{(1)}^{(d)}(d-1)}{2\pi} + \frac{a_5(d-1)}{2} + \frac{\beta_{(1)}^{(d)}(d-1)}{2\pi} - \frac{d}{2} + \frac{1}{2}, \\
g_4 &= -\frac{a_1\alpha_{(1)}^{(d)}(d-1)}{2\pi} + \frac{a_1(d-1)}{2} - \frac{a_2\alpha_{(1)}^{(d)}(d^2-3d+2)}{2\pi} + \frac{a_2(d^2-3d+2)}{2} \\
&\quad + \frac{a_4\nu_{(1)}(d^2-2d+1)\sin(\alpha_{(1)}^{(d)})}{2\pi\nu_{(d)}} + \frac{a_4(d-1)}{2} - \frac{a_4(d-1)\sin(\beta_{(d)}^{(d)})}{2\pi\nu_{(d)}} \\
&\quad - \frac{a_4(d^2-2d+1)\sin(\beta_{(d)}^{(1)})}{2\pi\nu_{(d)}} + \frac{\beta_{(d)}^{(1)}(d-1)}{2\pi} - \frac{d}{2} + \frac{1}{2}, \\
g_5 &= -\frac{a_3\alpha_{(1)}^{(d)}(d-1)}{2\pi} + \frac{a_3(d-1)}{2} + \frac{a_5\nu_{(1)}(d-1)\sin(\alpha_{(1)}^{(d)})}{2\pi\nu_{(d)}} \\
&\quad + \frac{a_5}{2} - \frac{a_5(d-1)\sin(\beta_{(d)}^{(1)})}{2\pi\nu_{(d)}} - \frac{a_5\sin(\beta_{(d)}^{(d)})}{2\pi\nu_{(d)}} + \frac{\beta_{(d)}^{(d)}}{2\pi} - \frac{1}{2}.
\end{aligned}$$

C.2 Gradient expressions for \mathcal{W}_2

The space \mathcal{W}_2 is six-dimensional. A weight matrix for $d = 8$ can be parameterized as follows

$$\begin{bmatrix} a_1 & a_2 & a_2 & a_2 & a_2 & a_2 & a_3 & a_3 \\ a_2 & a_1 & a_2 & a_2 & a_2 & a_2 & a_3 & a_3 \\ a_2 & a_2 & a_1 & a_2 & a_2 & a_2 & a_3 & a_3 \\ a_2 & a_2 & a_2 & a_1 & a_2 & a_2 & a_3 & a_3 \\ a_2 & a_2 & a_2 & a_2 & a_1 & a_2 & a_3 & a_3 \\ a_2 & a_2 & a_2 & a_2 & a_2 & a_1 & a_3 & a_3 \\ a_4 & a_4 & a_4 & a_4 & a_4 & a_4 & a_5 & a_6 \\ a_4 & a_4 & a_4 & a_4 & a_4 & a_4 & a_6 & a_5 \end{bmatrix}.$$

The gradient entries, denoted by g_1, g_2, g_3, g_4, g_5 and g_6 , are:

$$\begin{aligned} g_1 = & \frac{a_1(d-2)}{2} + \frac{a_1(d^2-5d+6)\sin(\alpha_{(1)}^{(2)})}{2\pi} + \frac{a_1\nu_{(d-1)}(d-2)\sin(\alpha_{(1)}^{(d-1)})}{\pi\nu_{(1)}} - \frac{a_1(d-2)\sin(\beta_{(1)}^{(1)})}{2\pi\nu_{(1)}} \\ & - \frac{a_1(d-2)\sin(\beta_{(1)}^{(d-1)})}{\pi\nu_{(1)}} - \frac{a_1(d^2-5d+6)\sin(\beta_{(1)}^{(2)})}{2\pi\nu_{(1)}} - \frac{a_2\alpha_{(1)}^{(2)}(d^2-5d+6)}{2\pi} \\ & + \frac{a_2(d^2-5d+6)}{2} - \frac{a_4\alpha_{(1)}^{(d-1)}(d-2)}{\pi} + a_4(d-2) + \frac{\beta_{(1)}^{(1)}(d-2)}{2\pi} - \frac{d}{2} + 1, \end{aligned}$$

$$\begin{aligned} g_2 = & -\frac{a_1\alpha_{(1)}^{(2)}(d^2-5d+6)}{2\pi} + \frac{a_1(d^2-5d+6)}{2} - \frac{a_2\alpha_{(1)}^{(2)}(d^3-9d^2+26d-24)}{2\pi} \\ & + \frac{a_2(d^3-8d^2+21d-18)\sin(\alpha_{(1)}^{(2)})}{2\pi} + \frac{a_2(d^3-8d^2+21d-18)}{2} \\ & + \frac{a_2\nu_{(d-1)}(d^2-5d+6)\sin(\alpha_{(1)}^{(d-1)})}{\pi\nu_{(1)}} - \frac{a_2(d^2-5d+6)\sin(\beta_{(1)}^{(1)})}{2\pi\nu_{(1)}} \\ & - \frac{a_2(d^2-5d+6)\sin(\beta_{(1)}^{(d-1)})}{\pi\nu_{(1)}} - \frac{a_2(d^3-8d^2+21d-18)\sin(\beta_{(1)}^{(2)})}{2\pi\nu_{(1)}} \\ & - \frac{a_4\alpha_{(1)}^{(d-1)}(d^2-5d+6)}{\pi} + a_4(d^2-5d+6) + \frac{\beta_{(1)}^{(2)}(d^2-5d+6)}{2\pi} - \frac{d^2}{2} + \frac{5d}{2} - 3, \end{aligned}$$

$$\begin{aligned} g_3 = & -\frac{a_3\alpha_{(1)}^{(2)}(d^2-5d+6)}{\pi} + \frac{a_3(d^2-5d+6)\sin(\alpha_{(1)}^{(2)})}{\pi} \\ & + a_3(d^2-4d+4) + \frac{2a_3\nu_{(d-1)}(d-2)\sin(\alpha_{(1)}^{(d-1)})}{\pi\nu_{(1)}} - \frac{a_3(d-2)\sin(\beta_{(1)}^{(1)})}{\pi\nu_{(1)}} \\ & - \frac{2a_3(d-2)\sin(\beta_{(1)}^{(d-1)})}{\pi\nu_{(1)}} - \frac{a_3(d^2-5d+6)\sin(\beta_{(1)}^{(2)})}{\pi\nu_{(1)}} - \frac{a_5\alpha_{(1)}^{(d-1)}(d-2)}{\pi} \\ & + a_5(d-2) - \frac{a_6\alpha_{(1)}^{(d-1)}(d-2)}{\pi} + a_6(d-2) + \frac{\beta_{(1)}^{(d-1)}(d-2)}{\pi} - d + 2, \end{aligned}$$

$$\begin{aligned}
g_4 &= -\frac{a_1 \alpha_{(1)}^{(d-1)} (d-2)}{\pi} + a_1 (d-2) - \frac{a_2 \alpha_{(1)}^{(d-1)} (d^2 - 5d + 6)}{\pi} + a_2 (d^2 - 5d + 6) - \frac{a_4 \alpha_{(d-1)}^{(d)} (d-2)}{\pi} \\
&+ \frac{a_4 \nu_{(1)} (d^2 - 4d + 4) \sin(\alpha_{(1)}^{(d-1)})}{\pi \nu_{(d-1)}} + \frac{a_4 (d-2) \sin(\alpha_{(d-1)}^{(d)})}{\pi} + 2a_4 (d-2) - \frac{a_4 (d-2) \sin(\beta_{(d-1)}^{(d)})}{\pi \nu_{(d-1)}} \\
&- \frac{a_4 (d-2) \sin(\beta_{(d-1)}^{(d-1)})}{\pi \nu_{(d-1)}} - \frac{a_4 (d^2 - 4d + 4) \sin(\beta_{(d-1)}^{(1)})}{\pi \nu_{(d-1)}} + \frac{\beta_{(d-1)}^{(1)} (d-2)}{\pi} - d + 2, \\
g_5 &= -\frac{a_3 \alpha_{(1)}^{(d-1)} (d-2)}{\pi} + a_3 (d-2) + \frac{a_5 \nu_{(1)} (d-2) \sin(\alpha_{(1)}^{(d-1)})}{\pi \nu_{(d-1)}} + \frac{a_5 \sin(\alpha_{(d-1)}^{(d)})}{\pi} + a_5 \\
&- \frac{a_5 (d-2) \sin(\beta_{(d-1)}^{(1)})}{\pi \nu_{(d-1)}} - \frac{a_5 \sin(\beta_{(d-1)}^{(d)})}{\pi \nu_{(d-1)}} - \frac{a_5 \sin(\beta_{(d-1)}^{(d-1)})}{\pi \nu_{(d-1)}} - \frac{a_6 \alpha_{(d-1)}^{(d)}}{\pi} + a_6 + \frac{\beta_{(d-1)}^{(d-1)}}{\pi} - 1 \\
g_6 &= -\frac{a_3 \alpha_{(1)}^{(d-1)} (d-2)}{\pi} + a_3 (d-2) - \frac{a_5 \alpha_{(d-1)}^{(d)}}{\pi} + a_5 + \frac{a_6 \nu_{(1)} (d-2) \sin(\alpha_{(1)}^{(d-1)})}{\pi \nu_{(d-1)}} + \frac{a_6 \sin(\alpha_{(d-1)}^{(d)})}{\pi} \\
&+ a_6 - \frac{a_6 (d-2) \sin(\beta_{(d-1)}^{(1)})}{\pi \nu_{(d-1)}} - \frac{a_6 \sin(\beta_{(d-1)}^{(d)})}{\pi \nu_{(d-1)}} - \frac{a_6 \sin(\beta_{(d-1)}^{(d-1)})}{\pi \nu_{(d-1)}} + \frac{\beta_{(d-1)}^{(d)}}{\pi} - 1.
\end{aligned}$$

C.3 Gradient expressions for \mathcal{W}_3

The space \mathcal{W}_3 is six-dimensional. A weight matrix for $d = 8$ can be parameterized as follows

$$\begin{bmatrix}
a_1 & a_2 & a_2 & a_2 & a_2 & a_3 & a_3 & a_3 \\
a_2 & a_1 & a_2 & a_2 & a_2 & a_3 & a_3 & a_3 \\
a_2 & a_2 & a_1 & a_2 & a_2 & a_3 & a_3 & a_3 \\
a_2 & a_2 & a_2 & a_1 & a_2 & a_3 & a_3 & a_3 \\
a_2 & a_2 & a_2 & a_2 & a_1 & a_3 & a_3 & a_3 \\
a_4 & a_4 & a_4 & a_4 & a_4 & a_5 & a_6 & a_6 \\
a_4 & a_4 & a_4 & a_4 & a_4 & a_6 & a_5 & a_6 \\
a_4 & a_4 & a_4 & a_4 & a_4 & a_6 & a_6 & a_5
\end{bmatrix}$$

The gradient entries, denoted by g_1, g_2, g_3, g_4, g_5 and g_6 , are:

$$\begin{aligned}
g_1 &= \frac{a_1(d-3)}{2} + \frac{a_1(d^2-7d+12)\sin(\alpha_{(1)}^{(2)})}{2\pi} + \frac{3a_1\nu_{(d-2)}(d-3)\sin(\alpha_{(1)}^{(d-2)})}{2\pi\nu_{(1)}} - \frac{a_1(d-3)\sin(\beta_{(1)}^{(1)})}{2\pi\nu_{(1)}} \\
&\quad - \frac{3a_1(d-3)\sin(\beta_{(1)}^{(d-2)})}{2\pi\nu_{(1)}} - \frac{a_1(d^2-7d+12)\sin(\beta_{(1)}^{(2)})}{2\pi\nu_{(1)}} - \frac{a_2\alpha_{(1)}^{(2)}(d^2-7d+12)}{2\pi} \\
&\quad + \frac{a_2(d^2-7d+12)}{2} - \frac{3a_4\alpha_{(1)}^{(d-2)}(d-3)}{2\pi} + \frac{3a_4(d-3)}{2} + \frac{\beta_{(1)}^{(1)}(d-3)}{2\pi} - \frac{d}{2} + \frac{3}{2}, \\
g_2 &= -\frac{a_1\alpha_{(1)}^{(2)}(d^2-7d+12)}{2\pi} + \frac{a_1(d^2-7d+12)}{2} - \frac{a_2\alpha_{(1)}^{(2)}(d^3-12d^2+47d-60)}{2\pi} \\
&\quad + \frac{a_2(d^3-11d^2+40d-48)\sin(\alpha_{(1)}^{(2)})}{2\pi} + \frac{a_2(d^3-11d^2+40d-48)}{2} \\
&\quad + \frac{3a_2\nu_{(d-2)}(d^2-7d+12)\sin(\alpha_{(1)}^{(d-2)})}{2\pi\nu_{(1)}} - \frac{a_2(d^2-7d+12)\sin(\beta_{(1)}^{(1)})}{2\pi\nu_{(1)}} \\
&\quad - \frac{3a_2(d^2-7d+12)\sin(\beta_{(1)}^{(d-2)})}{2\pi\nu_{(1)}} - \frac{a_2(d^3-11d^2+40d-48)\sin(\beta_{(1)}^{(2)})}{2\pi\nu_{(1)}} \\
&\quad - \frac{3a_4\alpha_{(1)}^{(d-2)}(d^2-7d+12)}{2\pi} + \frac{3a_4(d^2-7d+12)}{2} + \frac{\beta_{(1)}^{(2)}(d^2-7d+12)}{2\pi} - \frac{d^2}{2} + \frac{7d}{2} - 6, \\
g_3 &= -\frac{3a_3\alpha_{(1)}^{(2)}(d^2-7d+12)}{2\pi} + \frac{3a_3(d^2-7d+12)\sin(\alpha_{(1)}^{(2)})}{2\pi} + \frac{3a_3(d^2-6d+9)}{2} \\
&\quad + \frac{9a_3\nu_{(d-2)}(d-3)\sin(\alpha_{(1)}^{(d-2)})}{2\pi\nu_{(1)}} - \frac{3a_3(d-3)\sin(\beta_{(1)}^{(1)})}{2\pi\nu_{(1)}} - \frac{9a_3(d-3)\sin(\beta_{(1)}^{(d-2)})}{2\pi\nu_{(1)}} \\
&\quad - \frac{3a_3(d^2-7d+12)\sin(\beta_{(1)}^{(2)})}{2\pi\nu_{(1)}} - \frac{3a_5\alpha_{(1)}^{(d-2)}(d-3)}{2\pi} + \frac{3a_5(d-3)}{2} - \frac{3a_6\alpha_{(1)}^{(d-2)}(d-3)}{\pi} \\
&\quad + 3a_6(d-3) + \frac{3\beta_{(1)}^{(d-2)}(d-3)}{2\pi} - \frac{3d}{2} + \frac{9}{2},
\end{aligned}$$

$$\begin{aligned}
g_4 &= -\frac{3a_1\alpha_{(1)}^{(d-2)}(d-3)}{2\pi} + \frac{3a_1(d-3)}{2} - \frac{3a_2\alpha_{(1)}^{(d-2)}(d^2-7d+12)}{2\pi} \\
&+ \frac{3a_2(d^2-7d+12)}{2} - \frac{3a_4\alpha_{(d-2)}^{(d-1)}(d-3)}{\pi} + \frac{3a_4\nu_{(1)}(d^2-6d+9)\sin(\alpha_{(1)}^{(d-2)})}{2\pi\nu_{(d-2)}} \\
&+ \frac{3a_4(d-3)\sin(\alpha_{(d-2)}^{(d-1)})}{\pi} + \frac{9a_4(d-3)}{2} - \frac{3a_4(d-3)\sin(\beta_{(d-2)}^{(d-1)})}{\pi\nu_{(d-2)}} \\
&- \frac{3a_4(d-3)\sin(\beta_{(d-2)}^{(d-2)})}{2\pi\nu_{(d-2)}} - \frac{3a_4(d^2-6d+9)\sin(\beta_{(d-2)}^{(1)})}{2\pi\nu_{(d-2)}} + \frac{3\beta_{(d-2)}^{(1)}(d-3)}{2\pi} - \frac{3d}{2} + \frac{9}{2}, \\
g_5 &= -\frac{3a_3\alpha_{(1)}^{(d-2)}(d-3)}{2\pi} + \frac{3a_3(d-3)}{2} + \frac{3a_5\nu_{(1)}(d-3)\sin(\alpha_{(1)}^{(d-2)})}{2\pi\nu_{(d-2)}} + \frac{3a_5\sin(\alpha_{(d-2)}^{(d-1)})}{\pi} + \frac{3a_5}{2} \\
&- \frac{3a_5(d-3)\sin(\beta_{(d-2)}^{(1)})}{2\pi\nu_{(d-2)}} - \frac{3a_5\sin(\beta_{(d-2)}^{(d-1)})}{\pi\nu_{(d-2)}} - \frac{3a_5\sin(\beta_{(d-2)}^{(d-2)})}{2\pi\nu_{(d-2)}} - \frac{3a_6\alpha_{(d-2)}^{(d-1)}}{\pi} + 3a_6 + \frac{3\beta_{(d-2)}^{(d-2)}}{2\pi} - \frac{3}{2}, \\
g_6 &= -\frac{3a_3\alpha_{(1)}^{(d-2)}(d-3)}{\pi} + 3a_3(d-3) - \frac{3a_5\alpha_{(d-2)}^{(d-1)}}{\pi} + 3a_5 - \frac{3a_6\alpha_{(d-2)}^{(d-1)}}{\pi} + \frac{3a_6\nu_{(1)}(d-3)\sin(\alpha_{(1)}^{(d-2)})}{\pi\nu_{(d-2)}} \\
&+ \frac{6a_6\sin(\alpha_{(d-2)}^{(d-1)})}{\pi} + 6a_6 - \frac{3a_6(d-3)\sin(\beta_{(d-2)}^{(1)})}{\pi\nu_{(d-2)}} - \frac{6a_6\sin(\beta_{(d-2)}^{(d-1)})}{\pi\nu_{(d-2)}} \\
&- \frac{3a_6\sin(\beta_{(d-2)}^{(d-2)})}{\pi\nu_{(d-2)}} + \frac{3\beta_{(d-2)}^{(d-1)}}{\pi} - 3.
\end{aligned}$$

D Hessian spectrum

Below, we describe the technique we use to derive an analytic description of the Hessian spectrum. Some parts follow [3] verbatim. In order to avoid a long preliminaries section, key ideas and concepts are introduced and organized so as to illuminate our strategy for analyzing the Hessian. We illustrate with reference to the global minimum $W = V$ where $d = k$, the second layer is all ones, and the target weight matrix V is the identity I_d . In Section E, we provide the eigenvalue expressions for $\Delta(S_{d-1} \times S_1)$, organized by their isotypic component.

D.1 Studying invariance properties via group action

We first review background material on group actions and fix notations (see [20, Chapters 1, 2] for a more complete account). Elementary concepts from group theory are assumed known. We start with two examples that are used later.

Examples 1. (1) The *symmetric group* S_d , $d \in \mathbb{N}$, is the group of permutations of $[d] \doteq \{1, \dots, d\}$. (2) Let $\text{GL}(d, \mathbb{R})$ denote the space of invertible linear maps on \mathbb{R}^d . Under composition, $\text{GL}(d, \mathbb{R})$ has the structure of a group. The *orthogonal group* $\text{O}(d)$ is the subgroup of $\text{GL}(d, \mathbb{R})$ defined by $\text{O}(d) = \{A \in \text{GL}(d, \mathbb{R}) \mid \|Ax\| = \|x\|, \text{ for all } x \in \mathbb{R}^d\}$. Both $\text{GL}(d, \mathbb{R})$ and $\text{O}(d)$ can be viewed as groups of invertible $d \times d$ matrices.

Characteristically, these groups consist of *transformations* of a set and so we are led to the notion of a G -space X where we have an *action* of a group G on a set X . Formally, this is a group homomorphism from G to the group of bijections of X . For example, S_d naturally acts on $[d]$ as permutations and both $GL(d, \mathbb{R})$ and $O(d)$ act on \mathbb{R}^d as linear transformations (or matrix multiplication).

An example, which we use extensively in studying the invariance properties of \mathcal{L} , is given by the action of the group $S_k \times S_d \subset S_{k \times d}$, $k, d \in \mathbb{N}$, on $[k] \times [d]$ defined by

$$(\pi, \rho)(i, j) = (\pi^{-1}(i), \rho^{-1}(j)), \quad \pi \in S_k, \rho \in S_d, (i, j) \in [k] \times [d]. \quad (14)$$

This action induces an action on the space $M(k, d)$ of $k \times d$ -matrices $A = [A_{ij}]$ by $(\pi, \rho)[A_{ij}] = [A_{\pi^{-1}(i), \rho^{-1}(j)}]$. The action can be defined in terms of permutation matrices but is easier to describe in terms of rows and columns: $(\pi, \rho)A$ permutes rows (resp. columns) of A according to π (resp. ρ). As mentioned in the introduction, for our choice of $V = I_d$, \mathcal{L} is $S_k \times S_d$ -invariant. Note that $\Delta S_d \approx S_d$. When we restrict the $S_d \times S_d$ -action on $M(k, k)$ to ΔS_d , we refer to the diagonal S_d -action, or just the S_d -action on $M(d, d)$. This action of S_d on $M(d, d)$ maps diagonal matrices to diagonal matrices and should not be confused with the actions of S_d on $M(d, d)$ defined by either permuting rows or columns.

Example 2. Take $p, q \in \mathbb{N}$, $p + q = d$, and consider the diagonal action of $S_p \times S_q \subset S_d$ on $M(d, d)$.

Write $A \in M(d, d)$ in block matrix form as $A = \begin{bmatrix} A_{p,p} & A_{p,q} \\ A_{q,p} & A_{q,q} \end{bmatrix}$. If $(g, h) \in S_p \times S_q \subset S_d$, then

$(g, h)A = \begin{bmatrix} gA_{p,p} & (g, h)A_{p,q} \\ (h, g)A_{q,p} & hA_{q,q} \end{bmatrix}$ where $gA_{p,p}$ (resp. $hA_{q,q}$) are defined via the diagonal action of S_p (resp. S_q) on $A_{p,p}$ (resp. $A_{q,q}$), and $(g, h)A_{p,q}$ and $(h, g)A_{q,p}$ are defined through the natural action of $S_p \times S_q$ on rows and columns. Thus, for $(g, h)A_{p,q}$ (resp. $(h, g)A_{q,p}$) we permute rows (resp. columns) according to g and columns (resp. rows) according to h . In the case when $p = d - 1$, $q = 1$, S_{d-1} will act diagonally on $A_{d-1, d-1}$, fix a_{dd} , and act by permuting the first $(d - 1)$ entries of the last row and column.

As mentioned in body of the paper, given $W \in M(d, d)$, the largest subgroup of $S_d \times S_d$ fixing W is called the *isotropy* subgroup of W and is used as means of measuring the symmetry of W . The isotropy subgroup of $V \in M(d, d)$ is the diagonal subgroup ΔS_d . Our focus will be on critical points W whose isotropy groups are subgroups of the target matrix $V = I_d$, that is, ΔS_d and $\Delta(S_{d-1} \times S_1)$ (see [Figure 2](#)—we use the notation ΔS_d as the isotropy is a *subgroup* of $S_d \times S_d$). In the next section, we show how the symmetry of local minima greatly simplifies the analysis of their Hessian.

D.2 The spectrum of equivariant linear isomorphisms

If G is a subgroup of $O(d)$, the action on \mathbb{R}^d is called an *orthogonal* representation of G (we often drop the qualifier orthogonal). Denote by (\mathbb{R}^d, G) as necessary. The *degree* of a representation (V, G) is the dimension of V (V will always be a linear subspace of some \mathbb{R}^n with the induced Euclidean inner product). The action of $S_k \times S_d \subset S_{k \times d}$ on $M(k, d)$ is orthogonal with respect to the standard Euclidean inner product on $M(k, d) \approx \mathbb{R}^{k \times d}$ since the action permutes the coordinates of $\mathbb{R}^{k \times d}$ (equivalently, components of $k \times d$ matrices). Given two representations (V, G) and (W, G) , a map $A : V \rightarrow W$ is called G -equivariant if $A(gv) = gA(v)$, for all $g \in G, v \in V$. If A is linear and equivariant, we say A is a G -map. Invariant functions naturally provide examples of equivariant

maps. Thus the gradient $\nabla\mathcal{L}$ is a $S_k \times S_d$ -equivariant self map of $M(k, d)$ and if W is a critical point of $\nabla\mathcal{L}$ with isotropy $G \subset S_k \times S_d$, then $\nabla^2\mathcal{L}(W) : M(k, d) \rightarrow M(k, d)$ is a G -map (see [4]). The equivariance of the Hessian is the key ingredient that allows us to study the spectral density at *symmetric* local minima.

A representation (\mathbb{R}^n, G) is *irreducible* if the only linear subspaces of \mathbb{R}^n that are preserved (invariant) by the G -action are \mathbb{R}^n and $\{0\}$. Two orthogonal representations (V, G) , (W, G) are *isomorphic* (and have the same *isomorphism class*) if there exists a G -map $A : V \rightarrow W$ which is a linear isomorphism. If (V, G) , (W, G) are irreducible but not isomorphic then every G -map $A : V \rightarrow W$ is zero (as the kernel and the image of a G -map are G -invariant). If (V, G) is irreducible, then the space $\text{Hom}_G(V, V)$ of G -maps (endomorphisms) of V is a real associative division algebra and is isomorphic by a theorem of Frobenius to either \mathbb{R} , \mathbb{C} or \mathbb{H} (the quaternions). The *only* case that will concern us here is when $\text{Hom}_G(V, V) \approx \mathbb{R}$ when we say the representation is *real*.

Example 3. Let $n > 1$. Take the natural (orthogonal) action of S_n on \mathbb{R}^n defined by permuting coordinates. The representation is not irreducible since the subspace $T = \{(x, x, \dots, x) \in \mathbb{R}^n \mid x \in \mathbb{R}\}$ is invariant by the action of S_n , as is the hyperplane $H_{n-1} = T^\perp = \{(x_1, \dots, x_n) \mid \sum_{i \in [n]} x_i = 0\}$. It is easy to check that (T, S_n) , also called the *trivial* representation of S_n , and (H_{n-1}, S_n) , the *standard* representation, are irreducible, real, and not isomorphic.

Every representation (\mathbb{R}^n, G) can be written uniquely, up to order, as an orthogonal direct sum $\bigoplus_{i \in [m]} V_i$, where each (V_i, G) is an orthogonal direct sum of isomorphic irreducible representations (V_{ij}, G) , $j \in [p_i]$, and (V_{ij}, G) is isomorphic to $(V_{i'j'}, G)$ if and only if $i' = i$. The subspaces V_{ij} are *not* uniquely determined if $p_i > 1$. If there are m distinct isomorphism classes $\mathbf{v}_1, \dots, \mathbf{v}_m$ of irreducible representations, then (\mathbb{R}^n, G) may be represented by the sum $p_1\mathbf{v}_1 + \dots + p_m\mathbf{v}_m$, where $p_i \geq 1$ counts the number of representations with isomorphism class \mathbf{v}_i . Up to order, this sum (that is, the \mathbf{v}_i and their multiplicities) is uniquely determined by (\mathbb{R}^n, G) . This is the *isotypic decomposition* of (\mathbb{R}^n, G) (see [58]). The isotypic decomposition is a powerful tool for extracting information about the spectrum of G -maps.

If $G = S_d$, then every irreducible representation of S_d is real [21, Thm. 4.3]. Suppose, as above, that $(\mathbb{R}^n, S_d) = \bigoplus_{i \in [m]} V_i$ and $A : \mathbb{R}^n \rightarrow \mathbb{R}^n$ is an S_d -map. Since the induced maps $A_{ii'} : V_i \rightarrow V_{i'}$ must be zero if $i \neq i'$, A is uniquely determined by the S_d -maps $A_{ii} : V_i \rightarrow V_i$, $i \in [m]$. Fix i and choose an S_d -representation (W, S_d) in the isomorphism class \mathbf{v}_i . Choose S_d -isomorphisms $W \rightarrow V_{ij}$, $j \in [p_i]$. Then A_{ii} induces $\bar{A}_{ii} : W^{p_i} \rightarrow W^{p_i}$ and so determines a (real) matrix $M_i \in M(p_i, p_i)$ since $\text{Hom}_{S_d}(W, W) \approx \mathbb{R}$. Different choices of V_{ij} , or isomorphism $W \rightarrow V_{ij}$, yield a matrix similar to M_i . Each eigenvalue of M_i of multiplicity r gives an eigenvalue of A_{ii} , and so of A , of multiplicity $r \text{ degree}(\mathbf{v}_i)$.

Fact 1. (Notations and assumptions as above.) If A is the Hessian, all eigenvalues are real and each eigenvalue of M_i of multiplicity r will be an eigenvalue of A with multiplicity $r \text{ degree}(\mathbf{v}_i)$. In particular, A has most $\sum_{i \in [m]} p_i$ distinct real eigenvalues—regardless of the dimension of the underlying space.

Our strategy can be now summarized as follows. Given a local minima W , we compute the isotropy group $G \subset S_k \times S_d$ of W . Since the Hessian of \mathcal{F} at W is a G -map, may use the isotypic decomposition of the action of G on $M(k, d)$ to extract the spectral properties of the Hessian. In our setting, local minima have large isotropy groups, typically, as large as $\Delta(S_p \times S_{d-p})$, $0 \leq p <$

$d/2$. Studying the Hessian at these minima requires the isotopic decomposition corresponding to $\Delta(S_p \times S_{d-p})$, $0 \leq p < d/2$, which we detail in [Theorem D.3](#) below.

D.3 The isotypic decomposition of $(M(d, d), S_d)$ and the spectrum at $W = V$

Regard $M(d, d)$ as an S_d -space (diagonal action). The trivial representation, denoted by \mathfrak{t}_d , and the standard representation, denoted by \mathfrak{s}_d , introduced in [Example 3](#) are examples of the many irreducible representations of S_d . In the general theory, each irreducible representation of S_d is associated to a partition of the set $[d]$. The description of the isotypic decomposition of $(M(d, d), S_d)$ is relatively simple and uses just 4 irreducible representations of S_d for $d \geq 4$.

- The trivial representation \mathfrak{t}_d of degree 1.
- The standard representation \mathfrak{s}_d of S_d of degree $k - 1$.
- The exterior square representation $\mathfrak{r}_d = \wedge^2 \mathfrak{s}_d$ of degree $\frac{(d-1)(d-2)}{2}$.
- A representation \mathfrak{h}_d of degree $\frac{d(d-3)}{2}$. We describe \mathfrak{h}_d explicitly later in terms of symmetric matrices (formally, it is the representation associated to the partition $(d - 2, 2)$).

We omit the subscript d when clear from the context. Assume that $d \geq 4$. We begin with a well-known result about the representation $\mathfrak{s} \otimes \mathfrak{s}$ (see, e.g., [\[21\]](#)). If $\mathfrak{s} \odot \mathfrak{s}$ denotes the symmetric tensor product of \mathfrak{s} , then

$$\mathfrak{s} \otimes \mathfrak{s} = \mathfrak{s} \odot \mathfrak{s} + \mathfrak{r} = \mathfrak{t} + \mathfrak{s} + \mathfrak{h} + \mathfrak{r}. \quad (15)$$

Since all the irreducible S_d -representations are real, they are isomorphic to their dual representations and so we have the isotypic decomposition

$$M(k, k) \approx \mathbb{R}^k \otimes \mathbb{R}^k \approx (\mathfrak{s} + \mathfrak{t}) \otimes (\mathfrak{s} + \mathfrak{t}) = 2\mathfrak{t} + 3\mathfrak{s} + \mathfrak{r} + \mathfrak{h}, \quad (16)$$

since $\mathfrak{t} \otimes \mathfrak{s} = \mathfrak{s}$ and $\mathfrak{t} \otimes \mathfrak{t} = \mathfrak{t}$.

Using [Fact 1](#), information can immediately be deduced from [Equation \(16\)](#). For example, if W is a critical point of isotropy ΔS_d (a fixed point of the S_d -action on $M(d, d)$), then the spectrum of the Hessian contains at most $2 + 3 + 1 + 1 = 7$ distinct eigenvalues which distribute as follows: \mathfrak{t} contributes 2 eigenvalues of multiplicity 1, \mathfrak{s} contributes 2 eigenvalues of multiplicity $d - 1$, \mathfrak{r} contributes one eigenvalue of multiplicity $\frac{(d-1)(d-2)}{2}$, and \mathfrak{h} contributes one eigenvalue of multiplicity $\frac{d(d-3)}{2}$. This applies to the global minimum $W = V$ and the spurious minimum of type A.

Next, we would like to compute the actual eigenvalues. We demonstrate the method for the single \mathfrak{r} -eigenvalue (the example given in the body of the paper in [Section 4.2](#) refers to the single \mathfrak{h} -eigenvalue). Pick a non-zero vector from the \mathfrak{r} -representation. For example,

$$\mathfrak{X}^d = \begin{bmatrix} 0 & 1 & \dots & 1 & -(d-2) \\ -1 & 0 & \dots & 0 & 1 \\ \dots & \dots & \dots & \dots & \dots \\ -1 & 0 & \dots & 0 & 1 \\ (d-2) & -1 & \dots & -1 & 0 \end{bmatrix},$$

where rows and columns sum to zero and the only non-zero entries are in rows and columns 1 and d . Let $\overline{\mathfrak{X}}^d \in \mathbb{R}^{d \times d}$ be defined by concatenating the rows of \mathfrak{X}^d . Since \mathfrak{r} only occurs once in the

isotypic decomposition and $\nabla^2\mathcal{L}(V)$ is S_d -equivariant, $\overline{\mathfrak{X}}^d$ must be an eigenvector. In particular, $(\nabla^2\mathcal{L}(V)\overline{\mathfrak{X}}^d)_i = \lambda_{\mathfrak{r}}\overline{\mathfrak{X}}_i^d$, all $i \in [d^2]$. Choose i so that $\overline{\mathfrak{X}}_i^d \neq 0$. For example, $\overline{\mathfrak{X}}_2^d = 1$. Matrix multiplication, yields $\lambda_{\mathfrak{r}} = 1/4 - 1/2\pi$. A similar analysis holds for the eigenvalue associated to \mathfrak{r} . The multiple factors $2\mathfrak{t}$ and $3\mathfrak{s}$ are handled by making judicious choices of orthogonal invariant subspaces and representative vectors in $M(k, k)$.

Having described the general strategy for analyzing the Hessian spectrum for global minima, we now examine the spectrum at various types of spurious minima. We need two additional ingredients: a specification of the entries of a given family of spurious minima and the respective isotypic decomposition; we begin with the latter.

As discussed in the body of the paper, the symmetry-based analysis of the Hessian relies on the fact that isotropy groups of spurious minima tend to be (and some provably are) maximal subgroups of the target matrix isotropy. For $V = I$, the relevant maximal isotropy groups are of the form $\Delta(S_p \times S_q)$, $p + q = d$. Below, we provide the corresponding isotypic decomposition. Assume $d = k$ and regard $M(d, d)$ as an $S_p \times S_q$ -space, where $S_p \times S_q \subset S_d$ and the (diagonal) action of S_d is restricted to the subgroup $S_p \times S_q$.

Theorem ([3, Theorem 4]). *The isotypic decomposition of $(M(d, d), S_p \times S_q)$ is given by:*

1. *If $p = d - 1$, $q = 1$, and $k \geq 5$,*

$$M(d, d) = 5\mathfrak{t} + 5\mathfrak{s}_{d-1} + \mathfrak{r}_{d-1} + \mathfrak{r}_{d-1}.$$

2. *If $q \geq 2$, $d - 1 > p > p/2$ and $d \geq 4 + q$, then*

$$M(d, d) = 6\mathfrak{t} + 5\mathfrak{s}_p + a\mathfrak{s}_q + \mathfrak{r}_p + \mathfrak{r}_p + b\mathfrak{r}_q + c\mathfrak{r}_q + 2\mathfrak{s}_p \boxtimes \mathfrak{s}_q,$$

where if $q = 2$, then $a = 4, b = c = 0$; if $q = 3$, then $a = 5, b = 1, c = 0$; and if $q \geq 4$, then $a = 5, b = c = 1$.

(There is a minor error in [3, Theorem 4]. The correct value for a in the second case is as stated here.)

In contrast to the setting considered in [3], in our case the second layer is trainable. To compute the isotypic decomposition corresponding to this case (i.e., $M(d, d) \times \mathbb{R}^d$), we simply treat the weights of the second layer as an additional row of the weight matrix of the first layer. The additional row is split into p entries and $d - p$ entries. This adds $\mathfrak{t} + \mathfrak{s}_p$ to the isotypic decomposition if $q = 0$, $2\mathfrak{t} + \mathfrak{s}_p$ to the isotypic decomposition if $q = 1$, and $2\mathfrak{t} + \mathfrak{s}_p + \mathfrak{s}_q$ otherwise.

Theorem 4. *The isotypic decomposition of $(M(d, d), S_p \times S_q) \otimes (\mathbb{R}^d, S_p \times S_q)$ is given by:*

1. *If $p = d$, $q = 0$, and $k \geq 5$,*

$$M(d, d) = 3\mathfrak{t} + 4\mathfrak{s}_d + \mathfrak{r}_d + \mathfrak{r}_d.$$

2. *If $p = d - 1$, $q = 1$, and $k \geq 5$,*

$$M(d, d) = 7\mathfrak{t} + 6\mathfrak{s}_{d-1} + \mathfrak{r}_{d-1} + \mathfrak{r}_{d-1}.$$

3. If $q \geq 2$, $d - 1 > p > p/2$ and $d \geq 4 + q$, then

$$M(d, d) = 8\mathfrak{t} + 6\mathfrak{s}_p + a\mathfrak{s}_q + \mathfrak{r}_p + \mathfrak{r}_q + b\mathfrak{r}_q + c\mathfrak{r}_q + 2\mathfrak{s}_p \boxtimes \mathfrak{s}_q,$$

where if $q = 2$, then $a = 5, b = c = 0$; if $q = 3$, then $a = 6, b = 1, c = 0$; and if $q \geq 4$, then $a = 6, b = c = 1$.

Theorem 4 implies that the Hessian spectrum of local minima (or critical points) with isotropy $\Delta(S_p \times S_q)$ has at most 9 distinct eigenvalues if (1) applies, at most 15 distinct eigenvalues if (2) applies, and if (3) holds, at most 24 distinct eigenvalues if $q = 2$, at most 25 distinct eigenvalues if $q = 3$, and at most 26 distinct eigenvalues if $q \geq 4$. We omit some less interesting cases when k is small.

Following the same lines of argument described in [Section D.3](#), the next step is to pick a set of non-zero representative vectors for each irreducible representation that will allow us to compute the spectrum. We adopt the same of choice of representative vectors from [\[3\]](#). We demonstrate the final step with respect to the two trivial factors of S_d in [\(16\)](#). Let \mathfrak{D}_1 and \mathfrak{D}_2 be the two representatives and let $\nabla^2 \mathcal{L}(\mathfrak{D}_i) = \alpha_{i1} \mathfrak{D}_1 + \alpha_{i2} \mathfrak{D}_2$, $i = 1, 2$. The eigenvalues of $\nabla^2 \mathcal{L}|_{2\mathfrak{t}}$ are then the eigenvalues of the 2×2 transition matrix $A = [\alpha_{ij}]$. To compute the eigenvalues of A to, say, $O(d^{-1/2})$ -order, one solves the equation

$$\det(A - (x_1 d + x_2 d^{1/2} + x^3)) = 0,$$

for x_1, x_2, x_3 , where sufficiently many coefficients of the power series of the entries of A are assumed known. The same recipe is used for computing the rest of the eigenvalues.

E Eigenvalues transition matrices

Below, we provide the explicit form of the eigenvalue transition matrices for the natural representation of S_d .

r-rep. Let the associated 1×1 transition matrix be denoted by $T^{\mathfrak{r}}$. Then,

$$\begin{aligned} T_{1,1}^{\mathfrak{r}} = & -\frac{a_1^2}{2\pi\nu_{(1)}^2\nu_{(1)}^{(2)}} + \frac{a_1^2 \sin(\alpha_{(1)}^{(2)})}{2\pi\nu_{(1)}^2(\nu_{(1)}^{(2)})^2} + \frac{a_1 a_2}{\pi\nu_{(1)}^2\nu_{(1)}^{(2)}} - \frac{a_1 a_2 \sin(\alpha_{(1)}^{(2)})}{\pi\nu_{(1)}^2(\nu_{(1)}^{(2)})^2} - \frac{a_2^2}{2\pi\nu_{(1)}^2\nu_{(1)}^{(2)}} + \frac{a_2^2 \sin(\alpha_{(1)}^{(2)})}{2\pi\nu_{(1)}^2(\nu_{(1)}^{(2)})^2} \\ & + \frac{\alpha_{(1)}^{(2)}}{2\pi} + \frac{(d-1) \sin(\alpha_{(1)}^{(2)})}{2\pi} - \frac{(d-1) \sin(\beta_{(1)}^{(2)})}{2\pi\nu_{(1)}} - \frac{\sin(\beta_{(1)}^{(1)})}{2\pi\nu_{(1)}} - \frac{\sin(\beta_{(1)}^{(2)})}{2\pi(\mu_{(1)}^{(2)})^2\nu_{(1)}}. \end{aligned}$$

\eta-rep. Let the associated 1×1 transition matrix be denoted by $T^{\mathfrak{\eta}}$. Then,

$$\begin{aligned} T_{1,1}^{\mathfrak{\eta}} = & \frac{a_1^2}{2\pi\nu_{(1)}^2\nu_{(1)}^{(2)}} + \frac{a_1^2 \sin(\alpha_{(1)}^{(2)})}{2\pi\nu_{(1)}^2(\nu_{(1)}^{(2)})^2} - \frac{a_1 a_2}{\pi\nu_{(1)}^2\nu_{(1)}^{(2)}} - \frac{a_1 a_2 \sin(\alpha_{(1)}^{(2)})}{\pi\nu_{(1)}^2(\nu_{(1)}^{(2)})^2} + \frac{a_2^2}{2\pi\nu_{(1)}^2\nu_{(1)}^{(2)}} + \frac{a_2^2 \sin(\alpha_{(1)}^{(2)})}{2\pi\nu_{(1)}^2(\nu_{(1)}^{(2)})^2} \\ & + \frac{\alpha_{(1)}^{(2)}}{2\pi} + \frac{(d-1) \sin(\alpha_{(1)}^{(2)})}{2\pi} - \frac{(d-1) \sin(\beta_{(1)}^{(2)})}{2\pi\nu_{(1)}} - \frac{\sin(\beta_{(1)}^{(1)})}{2\pi\nu_{(1)}} - \frac{\sin(\beta_{(1)}^{(2)})}{2\pi(\mu_{(1)}^{(2)})^2\nu_{(1)}}. \end{aligned}$$

s-rep. Let the associated 4×4 transition matrix be denoted by T^s . Then,

$$\begin{aligned}
T_{1,1}^s = & -\frac{a_1^2 (d-1) \sin(\alpha_{(1)}^{(2)})}{2\pi\nu_{(1)}^2} - \frac{a_1^2}{2\pi\nu_{(1)}^2\nu_{(1)}^{(2)}} + \frac{a_1^2 (d-1) \sin(\alpha_{(1)}^{(2)}) \cos^2(\alpha_{(1)}^{(2)})}{2\pi\nu_{(1)}^2 (\nu_{(1)}^{(2)})^2} \\
& + \frac{a_1^2 (d-1) \sin(\beta_{(1)}^{(2)})}{2\pi\nu_{(1)}^3} + \frac{a_1^2 \sin(\beta_{(1)}^{(1)})}{2\pi\nu_{(1)}^3} - \frac{a_1^2 (d-1) \sin(\beta_{(1)}^{(2)}) \cos^2(\beta_{(1)}^{(2)})}{2\pi (\mu_{(1)}^{(2)})^2 \nu_{(1)}^3} \\
& - \frac{a_1^2 \sin(\beta_{(1)}^{(1)}) \cos^2(\beta_{(1)}^{(1)})}{2\pi (\mu_{(1)}^{(1)})^2 \nu_{(1)}^3} + \frac{a_1 a_2 \cos(\alpha_{(1)}^{(2)})}{\pi\nu_{(1)}^2\nu_{(1)}^{(2)}} - \frac{a_1 a_2 (d-1) \sin(\alpha_{(1)}^{(2)}) \cos(\alpha_{(1)}^{(2)})}{\pi\nu_{(1)}^2 (\nu_{(1)}^{(2)})^2} \\
& + \frac{a_1 \sin(\beta_{(1)}^{(1)}) \cos(\beta_{(1)}^{(1)})}{\pi (\mu_{(1)}^{(1)})^2 \nu_{(1)}^2} - \frac{a_2^2}{2\pi\nu_{(1)}^2\nu_{(1)}^{(2)}} + \frac{a_2^2 (d-1) \sin(\alpha_{(1)}^{(2)})}{2\pi\nu_{(1)}^2 (\nu_{(1)}^{(2)})^2} \\
& + \frac{(d-1) \sin(\alpha_{(1)}^{(2)})}{2\pi} + \frac{1}{2} - \frac{(d-1) \sin(\beta_{(1)}^{(2)})}{2\pi\nu_{(1)}} - \frac{\sin(\beta_{(1)}^{(1)})}{2\pi\nu_{(1)}} - \frac{\sin(\beta_{(1)}^{(1)})}{2\pi (\mu_{(1)}^{(1)})^2 \nu_{(1)}},
\end{aligned}$$

$$\begin{aligned}
T_{1,2}^s = & \frac{a_1^2 d \cos(\alpha_{(1)}^{(2)})}{2\pi\nu_{(1)}^2\nu_{(1)}^{(2)}} - \frac{a_1^2 d \sin(\alpha_{(1)}^{(2)}) \cos(\alpha_{(1)}^{(2)})}{2\pi\nu_{(1)}^2 (\nu_{(1)}^{(2)})^2} - \frac{a_1 a_2 d}{\pi\nu_{(1)}^2\nu_{(1)}^{(2)}} + \frac{a_1 a_2 d \sin(\alpha_{(1)}^{(2)})}{2\pi\nu_{(1)}^2 (\nu_{(1)}^{(2)})^2} \\
& + \frac{a_1 a_2 d \sin(\beta_{(1)}^{(1)})}{2\pi\nu_{(1)}^3} - \frac{a_1 a_2 d \sin(\beta_{(1)}^{(1)}) \cos^2(\beta_{(1)}^{(1)})}{2\pi (\mu_{(1)}^{(1)})^2 \nu_{(1)}^3} - \frac{a_1 a_2 (d^2 - d) \sin(\alpha_{(1)}^{(2)})}{2\pi\nu_{(1)}^2} \\
& - \frac{a_1 a_2 (d^2 - 2d) \sin(\alpha_{(1)}^{(2)}) \cos(\alpha_{(1)}^{(2)})}{2\pi\nu_{(1)}^2 (\nu_{(1)}^{(2)})^2} + \frac{a_1 a_2 (d^2 - d) \sin(\alpha_{(1)}^{(2)}) \cos^2(\alpha_{(1)}^{(2)})}{2\pi\nu_{(1)}^2 (\nu_{(1)}^{(2)})^2} \\
& + \frac{a_1 a_2 (d^2 - d) \sin(\beta_{(1)}^{(2)})}{2\pi\nu_{(1)}^3} - \frac{a_1 a_2 (d^2 - d) \sin(\beta_{(1)}^{(2)}) \cos^2(\beta_{(1)}^{(2)})}{2\pi (\mu_{(1)}^{(2)})^2 \nu_{(1)}^3} \\
& + \frac{a_1 d \sin(\beta_{(1)}^{(2)}) \cos(\beta_{(1)}^{(2)})}{2\pi (\mu_{(1)}^{(2)})^2 \nu_{(1)}^2} + \frac{a_2^2 d \cos(\alpha_{(1)}^{(2)})}{2\pi\nu_{(1)}^2\nu_{(1)}^{(2)}} + \frac{a_2^2 (d^2 - 2d) \sin(\alpha_{(1)}^{(2)})}{2\pi\nu_{(1)}^2 (\nu_{(1)}^{(2)})^2} \\
& - \frac{a_2^2 (d^2 - d) \sin(\alpha_{(1)}^{(2)}) \cos(\alpha_{(1)}^{(2)})}{2\pi\nu_{(1)}^2 (\nu_{(1)}^{(2)})^2} + \frac{a_2 d \sin(\beta_{(1)}^{(1)}) \cos(\beta_{(1)}^{(1)})}{2\pi (\mu_{(1)}^{(1)})^2 \nu_{(1)}^2} + \frac{\alpha_{(1)}^{(2)} d}{2\pi} - \frac{d}{2},
\end{aligned}$$

$$\begin{aligned}
T_{1,3}^s = & -\frac{a_1^2 (d-2) \cos(\alpha_{(1)}^{(2)})}{2\pi\nu_{(1)}^2\nu_{(1)}^{(2)}} - \frac{a_1^2 (d-2) \sin(\alpha_{(1)}^{(2)}) \cos(\alpha_{(1)}^{(2)})}{2\pi\nu_{(1)}^2 (\nu_{(1)}^{(2)})^2} - \frac{a_1 a_2 (d^2 - 3d + 2) \sin(\alpha_{(1)}^{(2)})}{2\pi\nu_{(1)}^2} \\
& + \frac{a_1 a_2 (d-2) \cos(\alpha_{(1)}^{(2)})}{\pi\nu_{(1)}^2\nu_{(1)}^{(2)}} + \frac{a_1 a_2 (d-2) \sin(\alpha_{(1)}^{(2)})}{2\pi\nu_{(1)}^2 (\nu_{(1)}^{(2)})^2} - \frac{a_1 a_2 (d^2 - 4d + 4) \sin(\alpha_{(1)}^{(2)}) \cos(\alpha_{(1)}^{(2)})}{2\pi\nu_{(1)}^2 (\nu_{(1)}^{(2)})^2} \\
& + \frac{a_1 a_2 (d^2 - 3d + 2) \sin(\alpha_{(1)}^{(2)}) \cos^2(\alpha_{(1)}^{(2)})}{2\pi\nu_{(1)}^2 (\nu_{(1)}^{(2)})^2} + \frac{a_1 a_2 (d-2) \sin(\beta_{(1)}^{(1)})}{2\pi\nu_{(1)}^3} \\
& + \frac{a_1 a_2 (d^2 - 3d + 2) \sin(\beta_{(1)}^{(2)})}{2\pi\nu_{(1)}^3} - \frac{a_1 a_2 (d^2 - 3d + 2) \sin(\beta_{(1)}^{(2)}) \cos^2(\beta_{(1)}^{(2)})}{2\pi (\mu_{(1)}^{(2)})^2 \nu_{(1)}^3} \\
& - \frac{a_1 a_2 (d-2) \sin(\beta_{(1)}^{(1)}) \cos^2(\beta_{(1)}^{(1)})}{2\pi (\mu_{(1)}^{(1)})^2 \nu_{(1)}^3} + \frac{a_1 (d-2) \sin(\beta_{(1)}^{(2)}) \cos(\beta_{(1)}^{(2)})}{2\pi (\mu_{(1)}^{(2)})^2 \nu_{(1)}^2} + \frac{a_2^2 (d-2) \cos(\alpha_{(1)}^{(2)})}{2\pi\nu_{(1)}^2\nu_{(1)}^{(2)}} \\
& - \frac{a_2^2 (d-2)}{\pi\nu_{(1)}^2\nu_{(1)}^{(2)}} + \frac{a_2^2 (d^2 - 4d + 4) \sin(\alpha_{(1)}^{(2)})}{2\pi\nu_{(1)}^2 (\nu_{(1)}^{(2)})^2} - \frac{a_2^2 (d^2 - 3d + 2) \sin(\alpha_{(1)}^{(2)}) \cos(\alpha_{(1)}^{(2)})}{2\pi\nu_{(1)}^2 (\nu_{(1)}^{(2)})^2} \\
& + \frac{a_2 (d-2) \sin(\beta_{(1)}^{(1)}) \cos(\beta_{(1)}^{(1)})}{2\pi (\mu_{(1)}^{(1)})^2 \nu_{(1)}^2} - \frac{\alpha_{(1)}^{(2)} (d-2)}{2\pi} + \frac{d}{2} - 1,
\end{aligned}$$

$$\begin{aligned}
T_{1,4}^s = & \frac{a_1 (d-2) \sin(\alpha_{(1)}^{(2)})}{2\pi} + a_1 - \frac{a_1 (d-1) \sin(\beta_{(1)}^{(2)})}{2\pi\nu_{(1)}} \\
& - \frac{a_1 \sin(\beta_{(1)}^{(1)})}{2\pi\nu_{(1)}} - \frac{a_2 \alpha_{(1)}^{(2)} (d-2)}{2\pi} + \frac{a_2 (d-2)}{2} + \frac{\beta_{(1)}^{(1)}}{2\pi} - \frac{1}{2},
\end{aligned}$$

$$\begin{aligned}
T_{2,1}^5 = & \frac{a_1^2 \cos(\alpha_{(1)}^{(2)})}{4\pi\nu_{(1)}^2\nu_{(1)}^{(2)}} - \frac{a_1^2 \sin(\alpha_{(1)}^{(2)}) \cos(\alpha_{(1)}^{(2)})}{4\pi\nu_{(1)}^2(\nu_{(1)}^{(2)})^2} - \frac{a_1 a_2 (d-1) \sin(\alpha_{(1)}^{(2)})}{4\pi\nu_{(1)}^2} - \frac{a_1 a_2}{2\pi\nu_{(1)}^2\nu_{(1)}^{(2)}} \\
& - \frac{a_1 a_2 (d-2) \sin(\alpha_{(1)}^{(2)}) \cos(\alpha_{(1)}^{(2)})}{4\pi\nu_{(1)}^2(\nu_{(1)}^{(2)})^2} + \frac{a_1 a_2 (d-1) \sin(\alpha_{(1)}^{(2)}) \cos^2(\alpha_{(1)}^{(2)})}{4\pi\nu_{(1)}^2(\nu_{(1)}^{(2)})^2} + \frac{a_1 a_2 \sin(\alpha_{(1)}^{(2)})}{4\pi\nu_{(1)}^2(\nu_{(1)}^{(2)})^2} \\
& + \frac{a_1 a_2 (d-1) \sin(\beta_{(1)}^{(2)})}{4\pi\nu_{(1)}^3} + \frac{a_1 a_2 \sin(\beta_{(1)}^{(1)})}{4\pi\nu_{(1)}^3} - \frac{a_1 a_2 (d-1) \sin(\beta_{(1)}^{(2)}) \cos^2(\beta_{(1)}^{(2)})}{4\pi(\mu_{(1)}^{(2)})^2\nu_{(1)}^3} \\
& - \frac{a_1 a_2 \sin(\beta_{(1)}^{(1)}) \cos^2(\beta_{(1)}^{(1)})}{4\pi(\mu_{(1)}^{(1)})^2\nu_{(1)}^3} + \frac{a_1 \sin(\beta_{(1)}^{(2)}) \cos(\beta_{(1)}^{(2)})}{4\pi(\mu_{(1)}^{(2)})^2\nu_{(1)}^2} + \frac{a_2^2 \cos(\alpha_{(1)}^{(2)})}{4\pi\nu_{(1)}^2\nu_{(1)}^{(2)}} + \frac{a_2^2 (d-2) \sin(\alpha_{(1)}^{(2)})}{4\pi\nu_{(1)}^2(\nu_{(1)}^{(2)})^2} \\
& - \frac{a_2^2 (d-1) \sin(\alpha_{(1)}^{(2)}) \cos(\alpha_{(1)}^{(2)})}{4\pi\nu_{(1)}^2(\nu_{(1)}^{(2)})^2} + \frac{a_2 \sin(\beta_{(1)}^{(1)}) \cos(\beta_{(1)}^{(1)})}{4\pi(\mu_{(1)}^{(1)})^2\nu_{(1)}^2} + \frac{\alpha_{(1)}^{(2)}}{4\pi} - \frac{1}{4},
\end{aligned}$$

$$\begin{aligned}
T_{2,2}^5 = & -\frac{a_1^2}{2\pi\nu_{(1)}^2\nu_{(1)}^{(2)}} + \frac{a_1^2 \sin(\alpha_{(1)}^{(2)})}{2\pi\nu_{(1)}^2(\nu_{(1)}^{(2)})^2} + \frac{a_1 a_2 d \cos(\alpha_{(1)}^{(2)})}{2\pi\nu_{(1)}^2\nu_{(1)}^{(2)}} - \frac{a_1 a_2 d \sin(\alpha_{(1)}^{(2)}) \cos(\alpha_{(1)}^{(2)})}{2\pi\nu_{(1)}^2(\nu_{(1)}^{(2)})^2} \\
& - \frac{a_1 a_2 (d-2)}{2\pi\nu_{(1)}^2\nu_{(1)}^{(2)}} + \frac{a_1 a_2 (d-2) \sin(\alpha_{(1)}^{(2)})}{2\pi\nu_{(1)}^2(\nu_{(1)}^{(2)})^2} + \frac{a_2^2 d \sin(\beta_{(1)}^{(1)})}{4\pi\nu_{(1)}^3} - \frac{a_2^2 d \sin(\beta_{(1)}^{(1)}) \cos^2(\beta_{(1)}^{(1)})}{4\pi(\mu_{(1)}^{(1)})^2\nu_{(1)}^3} \\
& - \frac{a_2^2 (d^2 - d) \sin(\alpha_{(1)}^{(2)})}{4\pi\nu_{(1)}^2} - \frac{a_2^2}{2\pi\nu_{(1)}^2\nu_{(1)}^{(2)}} - \frac{a_2^2 (d^2 - 2d) \sin(\alpha_{(1)}^{(2)}) \cos(\alpha_{(1)}^{(2)})}{2\pi\nu_{(1)}^2(\nu_{(1)}^{(2)})^2} \\
& + \frac{a_2^2 (d^2 - d) \sin(\alpha_{(1)}^{(2)}) \cos^2(\alpha_{(1)}^{(2)})}{4\pi\nu_{(1)}^2(\nu_{(1)}^{(2)})^2} + \frac{a_2^2 (d^2 - 3d + 2) \sin(\alpha_{(1)}^{(2)})}{4\pi\nu_{(1)}^2(\nu_{(1)}^{(2)})^2} + \frac{a_2^2 (d^2 - d) \sin(\beta_{(1)}^{(2)})}{4\pi\nu_{(1)}^3} \\
& - \frac{a_2^2 (d^2 - d) \sin(\beta_{(1)}^{(2)}) \cos^2(\beta_{(1)}^{(2)})}{4\pi(\mu_{(1)}^{(2)})^2\nu_{(1)}^3} + \frac{a_2 d \sin(\beta_{(1)}^{(2)}) \cos(\beta_{(1)}^{(2)})}{2\pi(\mu_{(1)}^{(2)})^2\nu_{(1)}^2} - \frac{\alpha_{(1)}^{(2)} (d-2)}{4\pi} \\
& + \frac{d}{4} + \frac{(d-1) \sin(\alpha_{(1)}^{(2)})}{2\pi} - \frac{(d-1) \sin(\beta_{(1)}^{(2)})}{2\pi\nu_{(1)}} - \frac{\sin(\beta_{(1)}^{(1)})}{2\pi\nu_{(1)}} - \frac{\sin(\beta_{(1)}^{(2)})}{2\pi(\mu_{(1)}^{(2)})^2\nu_{(1)}},
\end{aligned}$$

$$\begin{aligned}
T_{2,3}^5 = & -\frac{a_1 a_2 (d-2) \sin(\alpha_{(1)}^{(2)}) \cos(\alpha_{(1)}^{(2)})}{2\pi \nu_{(1)}^2 (\nu_{(1)}^{(2)})^2} + \frac{a_1 a_2 (d-2) \sin(\alpha_{(1)}^{(2)})}{2\pi \nu_{(1)}^2 (\nu_{(1)}^{(2)})^2} - \frac{a_2^2 (d^2 - 3d + 2) \sin(\alpha_{(1)}^{(2)})}{4\pi \nu_{(1)}^2} \\
& + \frac{a_2^2 (d-2) \cos(\alpha_{(1)}^{(2)})}{2\pi \nu_{(1)}^2 \nu_{(1)}^{(2)}} - \frac{a_2^2 (d-2)}{2\pi \nu_{(1)}^2 \nu_{(1)}^{(2)}} + \frac{a_2^2 (d^2 - 5d + 6) \sin(\alpha_{(1)}^{(2)})}{4\pi \nu_{(1)}^2 (\nu_{(1)}^{(2)})^2} \\
& - \frac{a_2^2 (d^2 - 4d + 4) \sin(\alpha_{(1)}^{(2)}) \cos(\alpha_{(1)}^{(2)})}{2\pi \nu_{(1)}^2 (\nu_{(1)}^{(2)})^2} + \frac{a_2^2 (d^2 - 3d + 2) \sin(\alpha_{(1)}^{(2)}) \cos^2(\alpha_{(1)}^{(2)})}{4\pi \nu_{(1)}^2 (\nu_{(1)}^{(2)})^2} \\
& + \frac{a_2^2 (d-2) \sin(\beta_{(1)}^{(1)})}{4\pi \nu_{(1)}^3} + \frac{a_2^2 (d^2 - 3d + 2) \sin(\beta_{(1)}^{(2)})}{4\pi \nu_{(1)}^3} - \frac{a_2^2 (d^2 - 3d + 2) \sin(\beta_{(1)}^{(2)}) \cos^2(\beta_{(1)}^{(2)})}{4\pi (\mu_{(1)}^{(2)})^2 \nu_{(1)}^3} \\
& - \frac{a_2^2 (d-2) \sin(\beta_{(1)}^{(1)}) \cos^2(\beta_{(1)}^{(1)})}{4\pi (\mu_{(1)}^{(1)})^2 \nu_{(1)}^3} + \frac{a_2 (d-2) \sin(\beta_{(1)}^{(2)}) \cos(\beta_{(1)}^{(2)})}{2\pi (\mu_{(1)}^{(2)})^2 \nu_{(1)}^2} + \frac{\alpha_{(1)}^{(2)} (d-2)}{4\pi} - \frac{d}{4} + \frac{1}{2},
\end{aligned}$$

$$T_{2,4}^5 = -\frac{a_2 \alpha_{(1)}^{(2)} (d-2)}{4\pi} + \frac{a_2 d}{4} + \frac{a_2 (d-2) \sin(\alpha_{(1)}^{(2)})}{4\pi} - \frac{a_2 (d-1) \sin(\beta_{(1)}^{(2)})}{4\pi \nu_{(1)}} - \frac{a_2 \sin(\beta_{(1)}^{(1)})}{4\pi \nu_{(1)}} + \frac{\beta_{(1)}^{(2)}}{4\pi} - \frac{1}{4},$$

$$\begin{aligned}
T_{3,1}^5 = & -\frac{a_1^2 \cos(\alpha_{(1)}^{(2)})}{4\pi \nu_{(1)}^2 \nu_{(1)}^{(2)}} - \frac{a_1^2 \sin(\alpha_{(1)}^{(2)}) \cos(\alpha_{(1)}^{(2)})}{4\pi \nu_{(1)}^2 (\nu_{(1)}^{(2)})^2} - \frac{a_1 a_2 (d-1) \sin(\alpha_{(1)}^{(2)})}{4\pi \nu_{(1)}^2} + \frac{a_1 a_2 \cos(\alpha_{(1)}^{(2)})}{2\pi \nu_{(1)}^2 \nu_{(1)}^{(2)}} \\
& - \frac{a_1 a_2 (d-2) \sin(\alpha_{(1)}^{(2)}) \cos(\alpha_{(1)}^{(2)})}{4\pi \nu_{(1)}^2 (\nu_{(1)}^{(2)})^2} + \frac{a_1 a_2 (d-1) \sin(\alpha_{(1)}^{(2)}) \cos^2(\alpha_{(1)}^{(2)})}{4\pi \nu_{(1)}^2 (\nu_{(1)}^{(2)})^2} + \frac{a_1 a_2 \sin(\alpha_{(1)}^{(2)})}{4\pi \nu_{(1)}^2 (\nu_{(1)}^{(2)})^2} \\
& + \frac{a_1 a_2 (d-1) \sin(\beta_{(1)}^{(2)})}{4\pi \nu_{(1)}^3} + \frac{a_1 a_2 \sin(\beta_{(1)}^{(1)})}{4\pi \nu_{(1)}^3} - \frac{a_1 a_2 (d-1) \sin(\beta_{(1)}^{(2)}) \cos^2(\beta_{(1)}^{(2)})}{4\pi (\mu_{(1)}^{(2)})^2 \nu_{(1)}^3} \\
& - \frac{a_1 a_2 \sin(\beta_{(1)}^{(1)}) \cos^2(\beta_{(1)}^{(1)})}{4\pi (\mu_{(1)}^{(1)})^2 \nu_{(1)}^3} + \frac{a_1 \sin(\beta_{(1)}^{(2)}) \cos(\beta_{(1)}^{(2)})}{4\pi (\mu_{(1)}^{(2)})^2 \nu_{(1)}^2} + \frac{a_2^2 \cos(\alpha_{(1)}^{(2)})}{4\pi \nu_{(1)}^2 \nu_{(1)}^{(2)}} - \frac{a_2^2}{2\pi \nu_{(1)}^2 \nu_{(1)}^{(2)}} \\
& + \frac{a_2^2 (d-2) \sin(\alpha_{(1)}^{(2)})}{4\pi \nu_{(1)}^2 (\nu_{(1)}^{(2)})^2} - \frac{a_2^2 (d-1) \sin(\alpha_{(1)}^{(2)}) \cos(\alpha_{(1)}^{(2)})}{4\pi \nu_{(1)}^2 (\nu_{(1)}^{(2)})^2} + \frac{a_2 \sin(\beta_{(1)}^{(1)}) \cos(\beta_{(1)}^{(1)})}{4\pi (\mu_{(1)}^{(1)})^2 \nu_{(1)}^2} - \frac{\alpha_{(1)}^{(2)}}{4\pi} + \frac{1}{4},
\end{aligned}$$

$$\begin{aligned}
T_{3,2}^5 = & -\frac{a_1 a_2 d \sin(\alpha_{(1)}^{(2)}) \cos(\alpha_{(1)}^{(2)})}{2\pi \nu_{(1)}^2 (\nu_{(1)}^{(2)})^2} + \frac{a_1 a_2 d \sin(\alpha_{(1)}^{(2)})}{2\pi \nu_{(1)}^2 (\nu_{(1)}^{(2)})^2} + \frac{a_2^2 d \cos(\alpha_{(1)}^{(2)})}{2\pi \nu_{(1)}^2 \nu_{(1)}^{(2)}} - \frac{a_2^2 d}{2\pi \nu_{(1)}^2 \nu_{(1)}^{(2)}} \\
& + \frac{a_2^2 d \sin(\beta_{(1)}^{(1)})}{4\pi \nu_{(1)}^3} - \frac{a_2^2 d \sin(\beta_{(1)}^{(1)}) \cos^2(\beta_{(1)}^{(1)})}{4\pi (\mu_{(1)}^{(1)})^2 \nu_{(1)}^3} - \frac{a_2^2 (d^2 - d) \sin(\alpha_{(1)}^{(2)})}{4\pi \nu_{(1)}^2} \\
& + \frac{a_2^2 (d^2 - 3d) \sin(\alpha_{(1)}^{(2)})}{4\pi \nu_{(1)}^2 (\nu_{(1)}^{(2)})^2} - \frac{a_2^2 (d^2 - 2d) \sin(\alpha_{(1)}^{(2)}) \cos(\alpha_{(1)}^{(2)})}{2\pi \nu_{(1)}^2 (\nu_{(1)}^{(2)})^2} \\
& + \frac{a_2^2 (d^2 - d) \sin(\alpha_{(1)}^{(2)}) \cos^2(\alpha_{(1)}^{(2)})}{4\pi \nu_{(1)}^2 (\nu_{(1)}^{(2)})^2} + \frac{a_2^2 (d^2 - d) \sin(\beta_{(1)}^{(2)})}{4\pi \nu_{(1)}^3} \\
& - \frac{a_2^2 (d^2 - d) \sin(\beta_{(1)}^{(2)}) \cos^2(\beta_{(1)}^{(2)})}{4\pi (\mu_{(1)}^{(2)})^2 \nu_{(1)}^3} + \frac{a_2 d \sin(\beta_{(1)}^{(2)}) \cos(\beta_{(1)}^{(2)})}{2\pi (\mu_{(1)}^{(2)})^2 \nu_{(1)}^2} + \frac{\alpha_{(1)}^{(2)} d}{4\pi} - \frac{d}{4},
\end{aligned}$$

$$\begin{aligned}
T_{3,3}^5 = & \frac{a_1^2}{2\pi \nu_{(1)}^2 \nu_{(1)}^{(2)}} + \frac{a_1^2 \sin(\alpha_{(1)}^{(2)})}{2\pi \nu_{(1)}^2 (\nu_{(1)}^{(2)})^2} + \frac{a_1 a_2 (d-4)}{2\pi \nu_{(1)}^2 \nu_{(1)}^{(2)}} - \frac{a_1 a_2 (d-2) \cos(\alpha_{(1)}^{(2)})}{2\pi \nu_{(1)}^2 \nu_{(1)}^{(2)}} \\
& + \frac{a_1 a_2 (d-4) \sin(\alpha_{(1)}^{(2)})}{2\pi \nu_{(1)}^2 (\nu_{(1)}^{(2)})^2} - \frac{a_1 a_2 (d-2) \sin(\alpha_{(1)}^{(2)}) \cos(\alpha_{(1)}^{(2)})}{2\pi \nu_{(1)}^2 (\nu_{(1)}^{(2)})^2} - \frac{a_2^2 (d^2 - 3d + 2) \sin(\alpha_{(1)}^{(2)})}{4\pi \nu_{(1)}^2} \\
& - \frac{a_2^2 (d - \frac{5}{2})}{\pi \nu_{(1)}^2 \nu_{(1)}^{(2)}} + \frac{a_2^2 (d-2) \cos(\alpha_{(1)}^{(2)})}{\pi \nu_{(1)}^2 \nu_{(1)}^{(2)}} + \frac{a_2^2 (d^2 - 5d + 8) \sin(\alpha_{(1)}^{(2)})}{4\pi \nu_{(1)}^2 (\nu_{(1)}^{(2)})^2} \\
& - \frac{a_2^2 (d^2 - 4d + 4) \sin(\alpha_{(1)}^{(2)}) \cos(\alpha_{(1)}^{(2)})}{2\pi \nu_{(1)}^2 (\nu_{(1)}^{(2)})^2} + \frac{a_2^2 (d^2 - 3d + 2) \sin(\alpha_{(1)}^{(2)}) \cos^2(\alpha_{(1)}^{(2)})}{4\pi \nu_{(1)}^2 (\nu_{(1)}^{(2)})^2} \\
& + \frac{a_2^2 (d-2) \sin(\beta_{(1)}^{(1)})}{4\pi \nu_{(1)}^3} + \frac{a_2^2 (d^2 - 3d + 2) \sin(\beta_{(1)}^{(2)})}{4\pi \nu_{(1)}^3} - \frac{a_2^2 (d^2 - 3d + 2) \sin(\beta_{(1)}^{(2)}) \cos^2(\beta_{(1)}^{(2)})}{4\pi (\mu_{(1)}^{(2)})^2 \nu_{(1)}^3} \\
& - \frac{a_2^2 (d-2) \sin(\beta_{(1)}^{(1)}) \cos^2(\beta_{(1)}^{(1)})}{4\pi (\mu_{(1)}^{(1)})^2 \nu_{(1)}^3} + \frac{a_2 (d-2) \sin(\beta_{(1)}^{(2)}) \cos(\beta_{(1)}^{(2)})}{2\pi (\mu_{(1)}^{(2)})^2 \nu_{(1)}^2} - \frac{\alpha_{(1)}^{(2)} (d-4)}{4\pi} \\
& + \frac{d}{4} + \frac{(d-1) \sin(\alpha_{(1)}^{(2)})}{2\pi} - \frac{1}{2} - \frac{(d-1) \sin(\beta_{(1)}^{(2)})}{2\pi \nu_{(1)}} - \frac{\sin(\beta_{(1)}^{(1)})}{2\pi \nu_{(1)}} - \frac{\sin(\beta_{(1)}^{(2)})}{2\pi (\mu_{(1)}^{(2)})^2 \nu_{(1)}},
\end{aligned}$$

$$T_{3,4}^5 = -\frac{a_1 \alpha_{(1)}^{(2)}}{2\pi} + \frac{a_1}{2} - \frac{a_2 \alpha_{(1)}^{(2)} (d-4)}{4\pi} + \frac{a_2 (d-2) \sin(\alpha_{(1)}^{(2)})}{4\pi} \\ + \frac{a_2 (d-2)}{4} - \frac{a_2 (d-1) \sin(\beta_{(1)}^{(2)})}{4\pi \nu_{(1)}} - \frac{a_2 \sin(\beta_{(1)}^{(1)})}{4\pi \nu_{(1)}} + \frac{\beta_{(1)}^{(2)}}{4\pi} - \frac{1}{4},$$

$$T_{4,1}^5 = \frac{a_1 (d-2) \sin(\alpha_{(1)}^{(2)})}{2\pi} + a_1 - \frac{a_1 (d-1) \sin(\beta_{(1)}^{(2)})}{2\pi \nu_{(1)}} \\ - \frac{a_1 \sin(\beta_{(1)}^{(1)})}{2\pi \nu_{(1)}} - \frac{a_2 \alpha_{(1)}^{(2)} (d-2)}{2\pi} + \frac{a_2 (d-2)}{2} + \frac{\beta_{(1)}^{(1)}}{2\pi} - \frac{1}{2},$$

$$T_{4,2}^5 = -\frac{a_2 \alpha_{(1)}^{(2)} (d^2 - 2d)}{2\pi} + \frac{a_2 d^2}{2} - \frac{a_2 d \sin(\beta_{(1)}^{(1)})}{2\pi \nu_{(1)}} \\ + \frac{a_2 (d^2 - 2d) \sin(\alpha_{(1)}^{(2)})}{2\pi} - \frac{a_2 (d^2 - d) \sin(\beta_{(1)}^{(2)})}{2\pi \nu_{(1)}} + \frac{\beta_{(1)}^{(2)} d}{2\pi} - \frac{d}{2},$$

$$T_{4,3}^5 = -\frac{a_1 \alpha_{(1)}^{(2)} (d-2)}{\pi} + a_1 (d-2) - \frac{a_2 \alpha_{(1)}^{(2)} (d^2 - 6d + 8)}{2\pi} + \frac{a_2 (d^2 - 4d + 4) \sin(\alpha_{(1)}^{(2)})}{2\pi} \\ + \frac{a_2 (d^2 - 4d + 4)}{2} - \frac{a_2 (d-2) \sin(\beta_{(1)}^{(1)})}{2\pi \nu_{(1)}} - \frac{a_2 (d^2 - 3d + 2) \sin(\beta_{(1)}^{(2)})}{2\pi \nu_{(1)}} + \frac{\beta_{(1)}^{(2)} (d-2)}{2\pi} - \frac{d}{2} + 1,$$

$$T_{4,4}^5 = \frac{\alpha_{(1)}^{(2)} \nu_{(1)}^2 \cos(\alpha_{(1)}^{(2)})}{2\pi} - \frac{\nu_{(1)}^2 \sin(\alpha_{(1)}^{(2)})}{2\pi} - \frac{\nu_{(1)}^2 \cos(\alpha_{(1)}^{(2)})}{2} + \frac{\nu_{(1)}^2}{2}.$$

t-rep. Let the associated 3×3 transition matrix be denoted by T^t . Then,

$$\begin{aligned}
T_{1,1}^t = & -\frac{a_1^2 (d-1) \sin(\alpha_{(1)}^{(2)})}{2\pi\nu_{(1)}^2} + \frac{a_1^2 (d-1)}{2\pi\nu_{(1)}^2\nu_{(1)}^{(2)}} + \frac{a_1^2 (d-1) \sin(\alpha_{(1)}^{(2)}) \cos^2(\alpha_{(1)}^{(2)})}{2\pi\nu_{(1)}^2 (\nu_{(1)}^{(2)})^2} \\
& + \frac{a_1^2 (d-1) \sin(\beta_{(1)}^{(2)})}{2\pi\nu_{(1)}^3} + \frac{a_1^2 \sin(\beta_{(1)}^{(1)})}{2\pi\nu_{(1)}^3} - \frac{a_1^2 (d-1) \sin(\beta_{(1)}^{(2)}) \cos^2(\beta_{(1)}^{(2)})}{2\pi (\mu_{(1)}^{(2)})^2 \nu_{(1)}^3} \\
& - \frac{a_1^2 \sin(\beta_{(1)}^{(1)}) \cos^2(\beta_{(1)}^{(1)})}{2\pi (\mu_{(1)}^{(1)})^2 \nu_{(1)}^3} - \frac{a_1 a_2 (d-1) \cos(\alpha_{(1)}^{(2)})}{\pi\nu_{(1)}^2\nu_{(1)}^{(2)}} - \frac{a_1 a_2 (d-1) \sin(\alpha_{(1)}^{(2)}) \cos(\alpha_{(1)}^{(2)})}{\pi\nu_{(1)}^2 (\nu_{(1)}^{(2)})^2} \\
& + \frac{a_1 \sin(\beta_{(1)}^{(1)}) \cos(\beta_{(1)}^{(1)})}{\pi (\mu_{(1)}^{(1)})^2 \nu_{(1)}^2} + \frac{a_2^2 (d-1)}{2\pi\nu_{(1)}^2\nu_{(1)}^{(2)}} + \frac{a_2^2 (d-1) \sin(\alpha_{(1)}^{(2)})}{2\pi\nu_{(1)}^2 (\nu_{(1)}^{(2)})^2} \\
& + \frac{(d-1) \sin(\alpha_{(1)}^{(2)})}{2\pi} + \frac{1}{2} - \frac{(d-1) \sin(\beta_{(1)}^{(2)})}{2\pi\nu_{(1)}} - \frac{\sin(\beta_{(1)}^{(1)})}{2\pi\nu_{(1)}} - \frac{\sin(\beta_{(1)}^{(1)})}{2\pi (\mu_{(1)}^{(1)})^2 \nu_{(1)}},
\end{aligned}$$

$$\begin{aligned}
T_{1,2}^t = & -\frac{a_1^2 (d-1) \cos(\alpha_{(1)}^{(2)})}{2\pi\nu_{(1)}^2\nu_{(1)}^{(2)}} - \frac{a_1^2 (d-1) \sin(\alpha_{(1)}^{(2)}) \cos(\alpha_{(1)}^{(2)})}{2\pi\nu_{(1)}^2 (\nu_{(1)}^{(2)})^2} - \frac{a_1 a_2 (d^2 - 2d + 1) \sin(\alpha_{(1)}^{(2)})}{2\pi\nu_{(1)}^2} \\
& + \frac{a_1 a_2 (d^2 - d)}{2\pi\nu_{(1)}^2\nu_{(1)}^{(2)}} - \frac{a_1 a_2 (d^2 - 3d + 2) \cos(\alpha_{(1)}^{(2)})}{2\pi\nu_{(1)}^2\nu_{(1)}^{(2)}} + \frac{a_1 a_2 (d-1) \sin(\alpha_{(1)}^{(2)})}{2\pi\nu_{(1)}^2 (\nu_{(1)}^{(2)})^2} \\
& - \frac{a_1 a_2 (d^2 - 3d + 2) \sin(\alpha_{(1)}^{(2)}) \cos(\alpha_{(1)}^{(2)})}{2\pi\nu_{(1)}^2 (\nu_{(1)}^{(2)})^2} + \frac{a_1 a_2 (d^2 - 2d + 1) \sin(\alpha_{(1)}^{(2)}) \cos^2(\alpha_{(1)}^{(2)})}{2\pi\nu_{(1)}^2 (\nu_{(1)}^{(2)})^2} \\
& + \frac{a_1 a_2 (d-1) \sin(\beta_{(1)}^{(1)})}{2\pi\nu_{(1)}^3} + \frac{a_1 a_2 (d^2 - 2d + 1) \sin(\beta_{(1)}^{(2)})}{2\pi\nu_{(1)}^3} \\
& - \frac{a_1 a_2 (d^2 - 2d + 1) \sin(\beta_{(1)}^{(2)}) \cos^2(\beta_{(1)}^{(2)})}{2\pi (\mu_{(1)}^{(2)})^2 \nu_{(1)}^3} - \frac{a_1 a_2 (d-1) \sin(\beta_{(1)}^{(1)}) \cos^2(\beta_{(1)}^{(1)})}{2\pi (\mu_{(1)}^{(1)})^2 \nu_{(1)}^3} \\
& + \frac{a_1 (d-1) \sin(\beta_{(1)}^{(2)}) \cos(\beta_{(1)}^{(2)})}{2\pi (\mu_{(1)}^{(2)})^2 \nu_{(1)}^2} + \frac{a_2^2 (d^2 - 3d + 2)}{2\pi\nu_{(1)}^2\nu_{(1)}^{(2)}} - \frac{a_2^2 (d^2 - 2d + 1) \cos(\alpha_{(1)}^{(2)})}{2\pi\nu_{(1)}^2\nu_{(1)}^{(2)}} \\
& + \frac{a_2^2 (d^2 - 3d + 2) \sin(\alpha_{(1)}^{(2)})}{2\pi\nu_{(1)}^2 (\nu_{(1)}^{(2)})^2} - \frac{a_2^2 (d^2 - 2d + 1) \sin(\alpha_{(1)}^{(2)}) \cos(\alpha_{(1)}^{(2)})}{2\pi\nu_{(1)}^2 (\nu_{(1)}^{(2)})^2} \\
& + \frac{a_2 (d-1) \sin(\beta_{(1)}^{(1)}) \cos(\beta_{(1)}^{(1)})}{2\pi (\mu_{(1)}^{(1)})^2 \nu_{(1)}^2} - \frac{\alpha_{(1)}^{(2)} (d-1)}{2\pi} + \frac{d}{2} - \frac{1}{2},
\end{aligned}$$

$$T_{1,3}^t = \frac{a_1 (d-1) \sin(\alpha_{(1)}^{(2)})}{\pi} + a_1 - \frac{a_1 (d-1) \sin(\beta_{(1)}^{(2)})}{2\pi\nu_{(1)}} - \frac{a_1 \sin(\beta_{(1)}^{(1)})}{2\pi\nu_{(1)}} - \frac{a_2 \alpha_{(1)}^{(2)} (d-1)}{\pi} + a_2 (d-1) + \frac{\beta_{(1)}^{(1)}}{2\pi} - \frac{1}{2},$$

$$T_{2,1}^t = -\frac{a_1^2 \cos(\alpha_{(1)}^{(2)})}{2\pi\nu_{(1)}^2 \nu_{(1)}^{(2)}} - \frac{a_1^2 \sin(\alpha_{(1)}^{(2)}) \cos(\alpha_{(1)}^{(2)})}{2\pi\nu_{(1)}^2 (\nu_{(1)}^{(2)})^2} + \frac{a_1 a_2 d}{2\pi\nu_{(1)}^2 \nu_{(1)}^{(2)}} - \frac{a_1 a_2 (d-1) \sin(\alpha_{(1)}^{(2)})}{2\pi\nu_{(1)}^2} - \frac{a_1 a_2 (d-2) \cos(\alpha_{(1)}^{(2)})}{2\pi\nu_{(1)}^2 \nu_{(1)}^{(2)}} - \frac{a_1 a_2 (d-2) \sin(\alpha_{(1)}^{(2)}) \cos(\alpha_{(1)}^{(2)})}{2\pi\nu_{(1)}^2 (\nu_{(1)}^{(2)})^2} + \frac{a_1 a_2 (d-1) \sin(\alpha_{(1)}^{(2)}) \cos^2(\alpha_{(1)}^{(2)})}{2\pi\nu_{(1)}^2 (\nu_{(1)}^{(2)})^2} + \frac{a_1 a_2 \sin(\alpha_{(1)}^{(2)})}{2\pi\nu_{(1)}^2 (\nu_{(1)}^{(2)})^2} + \frac{a_1 a_2 (d-1) \sin(\beta_{(1)}^{(2)})}{2\pi\nu_{(1)}^3} + \frac{a_1 a_2 \sin(\beta_{(1)}^{(1)})}{2\pi\nu_{(1)}^3} - \frac{a_1 a_2 (d-1) \sin(\beta_{(1)}^{(2)}) \cos^2(\beta_{(1)}^{(2)})}{2\pi (\mu_{(1)}^{(2)})^2 \nu_{(1)}^3} - \frac{a_1 a_2 \sin(\beta_{(1)}^{(1)}) \cos^2(\beta_{(1)}^{(1)})}{2\pi (\mu_{(1)}^{(1)})^2 \nu_{(1)}^3} + \frac{a_1 \sin(\beta_{(1)}^{(2)}) \cos(\beta_{(1)}^{(2)})}{2\pi (\mu_{(1)}^{(2)})^2 \nu_{(1)}^2} + \frac{a_2^2 (d-2)}{2\pi\nu_{(1)}^2 \nu_{(1)}^{(2)}} - \frac{a_2^2 (d-1) \cos(\alpha_{(1)}^{(2)})}{2\pi\nu_{(1)}^2 \nu_{(1)}^{(2)}} + \frac{a_2^2 (d-2) \sin(\alpha_{(1)}^{(2)})}{2\pi\nu_{(1)}^2 (\nu_{(1)}^{(2)})^2} - \frac{a_2^2 (d-1) \sin(\alpha_{(1)}^{(2)}) \cos(\alpha_{(1)}^{(2)})}{2\pi\nu_{(1)}^2 (\nu_{(1)}^{(2)})^2} + \frac{a_2 \sin(\beta_{(1)}^{(1)}) \cos(\beta_{(1)}^{(1)})}{2\pi (\mu_{(1)}^{(1)})^2 \nu_{(1)}^2} - \frac{\alpha_{(1)}^{(2)}}{2\pi} + \frac{1}{2},$$

$$\begin{aligned}
T_{2,2}^t = & \frac{a_1^2}{2\pi\nu_{(1)}^2\nu_{(1)}^{(2)}} + \frac{a_1^2 \sin(\alpha_{(1)}^{(2)})}{2\pi\nu_{(1)}^2(\nu_{(1)}^{(2)})^2} + \frac{a_1 a_2 (d-2)}{\pi\nu_{(1)}^2\nu_{(1)}^{(2)}} - \frac{a_1 a_2 (d-1) \cos(\alpha_{(1)}^{(2)})}{\pi\nu_{(1)}^2\nu_{(1)}^{(2)}} \\
& + \frac{a_1 a_2 (d-2) \sin(\alpha_{(1)}^{(2)})}{\pi\nu_{(1)}^2(\nu_{(1)}^{(2)})^2} - \frac{a_1 a_2 (d-1) \sin(\alpha_{(1)}^{(2)}) \cos(\alpha_{(1)}^{(2)})}{\pi\nu_{(1)}^2(\nu_{(1)}^{(2)})^2} - \frac{a_2^2 (d^2 - 2d + 1) \sin(\alpha_{(1)}^{(2)})}{2\pi\nu_{(1)}^2} \\
& - \frac{a_2^2 (d^2 - 3d + 2) \cos(\alpha_{(1)}^{(2)})}{\pi\nu_{(1)}^2\nu_{(1)}^{(2)}} + \frac{a_2^2 (d^2 - 3d + \frac{5}{2})}{\pi\nu_{(1)}^2\nu_{(1)}^{(2)}} + \frac{a_2^2 (d^2 - 4d + 4) \sin(\alpha_{(1)}^{(2)})}{2\pi\nu_{(1)}^2(\nu_{(1)}^{(2)})^2} \\
& - \frac{a_2^2 (d^2 - 3d + 2) \sin(\alpha_{(1)}^{(2)}) \cos(\alpha_{(1)}^{(2)})}{\pi\nu_{(1)}^2(\nu_{(1)}^{(2)})^2} + \frac{a_2^2 (d^2 - 2d + 1) \sin(\alpha_{(1)}^{(2)}) \cos^2(\alpha_{(1)}^{(2)})}{2\pi\nu_{(1)}^2(\nu_{(1)}^{(2)})^2} \\
& + \frac{a_2^2 (d-1) \sin(\beta_{(1)}^{(1)})}{2\pi\nu_{(1)}^3} + \frac{a_2^2 (d^2 - 2d + 1) \sin(\beta_{(1)}^{(2)})}{2\pi\nu_{(1)}^3} - \frac{a_2^2 (d^2 - 2d + 1) \sin(\beta_{(1)}^{(2)}) \cos^2(\beta_{(1)}^{(2)})}{2\pi(\mu_{(1)}^{(2)})^2\nu_{(1)}^3} \\
& - \frac{a_2^2 (d-1) \sin(\beta_{(1)}^{(1)}) \cos^2(\beta_{(1)}^{(1)})}{2\pi(\mu_{(1)}^{(1)})^2\nu_{(1)}^3} + \frac{a_2 (d-1) \sin(\beta_{(1)}^{(2)}) \cos(\beta_{(1)}^{(2)})}{\pi(\mu_{(1)}^{(2)})^2\nu_{(1)}^2} - \frac{\alpha_{(1)}^{(2)} (d-2)}{2\pi} \\
& + \frac{d}{2} + \frac{(d-1) \sin(\alpha_{(1)}^{(2)})}{2\pi} - \frac{1}{2} - \frac{(d-1) \sin(\beta_{(1)}^{(2)})}{2\pi\nu_{(1)}} - \frac{\sin(\beta_{(1)}^{(1)})}{2\pi\nu_{(1)}} - \frac{\sin(\beta_{(1)}^{(2)})}{2\pi(\mu_{(1)}^{(2)})^2\nu_{(1)}},
\end{aligned}$$

$$\begin{aligned}
T_{2,3}^t = & -\frac{a_1 \alpha_{(1)}^{(2)}}{\pi} + a_1 - \frac{a_2 \alpha_{(1)}^{(2)} (d-2)}{\pi} + \frac{a_2 (d-1) \sin(\alpha_{(1)}^{(2)})}{\pi} \\
& + a_2 (d-1) - \frac{a_2 (d-1) \sin(\beta_{(1)}^{(2)})}{2\pi\nu_{(1)}} - \frac{a_2 \sin(\beta_{(1)}^{(1)})}{2\pi\nu_{(1)}} + \frac{\beta_{(1)}^{(2)}}{2\pi} - \frac{1}{2},
\end{aligned}$$

$$\begin{aligned}
T_{3,1}^t = & \frac{a_1 (d-1) \sin(\alpha_{(1)}^{(2)})}{\pi} + a_1 - \frac{a_1 (d-1) \sin(\beta_{(1)}^{(2)})}{2\pi\nu_{(1)}} \\
& - \frac{a_1 \sin(\beta_{(1)}^{(1)})}{2\pi\nu_{(1)}} - \frac{a_2 \alpha_{(1)}^{(2)} (d-1)}{\pi} + a_2 (d-1) + \frac{\beta_{(1)}^{(1)}}{2\pi} - \frac{1}{2},
\end{aligned}$$

$$\begin{aligned}
T_{3,2}^t = & -\frac{a_1 \alpha_{(1)}^{(2)} (d-1)}{\pi} + a_1 (d-1) - \frac{a_2 \alpha_{(1)}^{(2)} (d^2 - 3d + 2)}{\pi} + \frac{a_2 (d^2 - 2d + 1) \sin(\alpha_{(1)}^{(2)})}{\pi} \\
& + a_2 (d^2 - 2d + 1) - \frac{a_2 (d-1) \sin(\beta_{(1)}^{(1)})}{2\pi\nu_{(1)}} - \frac{a_2 (d^2 - 2d + 1) \sin(\beta_{(1)}^{(2)})}{2\pi\nu_{(1)}} + \frac{\beta_{(1)}^{(2)} (d-1)}{2\pi} - \frac{d}{2} + \frac{1}{2},
\end{aligned}$$

$$T_{3,3}^t = -\frac{\alpha_{(1)}^{(2)} \nu_{(1)}^2 (d-1) \cos\left(\alpha_{(1)}^{(2)}\right)}{2\pi} + \frac{\nu_{(1)}^2 (d-1) \sin\left(\alpha_{(1)}^{(2)}\right)}{2\pi} + \frac{\nu_{(1)}^2 (d-1) \cos\left(\alpha_{(1)}^{(2)}\right)}{2} + \frac{\nu_{(1)}^2}{2}.$$

F Power series and Hessian spectrum by representation

We present the (fractional) power series of the minima described 1 to $O(d^{-5/2})$ -order, along with the respective eigenvalues arranged by their representation.

F.1 Theorem 1, case 2a

$$\begin{aligned} a_1 &= 1 + \frac{8}{\pi d^2} + O\left(d^{-\frac{5}{2}}\right), \\ a_2 &= -\frac{4}{\pi d^2} + O\left(d^{-\frac{5}{2}}\right), \\ a_3 &= \frac{2}{d} + \frac{-\frac{8}{\pi} - 2}{d^2} + O\left(d^{-\frac{5}{2}}\right), \\ a_4 &= \frac{4}{\pi d} + \frac{32}{\pi^3 d^{\frac{3}{2}}} + \frac{8(-7\pi^3 - 8\pi^2 + 64)}{\pi^5 d^2} + O\left(d^{-\frac{5}{2}}\right), \\ a_5 &= -1 + \frac{\frac{8}{\pi^2} + 2 + \frac{8}{\pi}}{d} + \frac{64(12 - \pi)}{3\pi^4 d^{\frac{3}{2}}(-2 + \pi)} \\ &\quad + \frac{2(-128\pi^3 - 40\pi^4 - 224\pi^2 - 512\pi + 2560 + \pi^7 + 10\pi^6 + 52\pi^5)}{\pi^6 d^2(-2 + \pi)} + O\left(d^{-\frac{5}{2}}\right). \end{aligned}$$

F.2 Eigenvalues

r-Representation	$\frac{(d-2)(d-3)}{2}$	$\frac{-2+\pi}{4\pi}$						
η-Representation	$\frac{(d-1)(d-4)}{2}$	$\frac{2+\pi}{4\pi}$						
Standard Representation	$d - 2$	0	$\frac{-2+\pi}{4\pi}$	$\frac{-2+\pi}{2\pi}$	$\frac{1}{4}$	$\frac{2+\pi}{4\pi}$	$\frac{d}{4} + \frac{1}{2}$	
Trivial Representation	1	0	0	$\frac{-2+\pi}{2\pi}$	$\frac{1}{4}$	$\frac{d}{4} + \frac{-4+\pi+\pi^2}{-8\pi+2\pi^2}$	$\frac{d}{4} + \frac{1}{2}$	$\frac{d}{\pi} + \frac{-10\pi+8+\pi^2}{2\pi(-4+\pi)}$

F.3 Theorem 1, case 2b

$$\begin{aligned}
a_1 &= -1 + \frac{2}{d} + -\frac{4(-16\pi^2 + (-2 + \pi)(-6\pi^3 + 16\pi + 8\pi^2 + \pi^4) + 32\pi)}{\pi^3 d^2 (-2 + \pi)^2} + O(d^{-\frac{5}{2}}), \\
a_2 &= \frac{2}{d} + \frac{-2 + \frac{8}{\pi}}{d^2} + O(d^{-\frac{5}{2}}), \\
a_3 &= -\frac{4(-32\pi + (-2 + \pi)(-10\pi^2 - 8\pi + 3\pi^3) + 16\pi^2)}{\pi^3 d^2 (-2 + \pi)^2} + O(d^{-\frac{5}{2}}), \\
a_4 &= \frac{2 - \frac{4}{\pi}}{d} + \frac{32(1 - \pi)}{\pi^3 d^{\frac{3}{2}}} + \frac{-\frac{136}{\pi^2} - \frac{128}{\pi^3} - 2 - \frac{512}{\pi^5} + \frac{768}{\pi^4} + \frac{52}{\pi}}{d^2} + O(d^{-\frac{5}{2}}), \\
a_5 &= 1 + \frac{8(-1 + \pi)}{\pi^2 d} + \\
&\quad \frac{2(-90\pi^3 - 792\pi + \pi\sqrt{-160\pi^3 - 12\pi^5 - 192\pi + 64 + \pi^6 + 240\pi^2 + 60\pi^4 + 384 + 11\pi^4 + 468\pi^2})}{3\pi^4 d^{\frac{3}{2}}(-2 + \pi)} \\
&\quad + \frac{h_4}{d^2} + O(d^{-\frac{5}{2}}).
\end{aligned}$$

F.4 Eigenvalues

r-Representation	$\frac{(d-2)(d-3)}{2}$	$\frac{-2+\pi}{4\pi}$						
η -Representation	$\frac{(d-1)(d-4)}{2}$	$\frac{2+\pi}{4\pi}$						
Standard Representation	$d - 2$	0	$\frac{-2+\pi}{4\pi}$	$\frac{-2+\pi}{2\pi}$	$\frac{1}{4}$	$\frac{2+\pi}{4\pi}$	$\frac{d}{4} + \frac{1}{2}$	
Trivial Representation	1	0	0	$\frac{-2+\pi}{2\pi}$	$\frac{1}{4}$	$\frac{d}{4} + \frac{-4+\pi+\pi^2}{-8\pi+2\pi^2}$	$\frac{d}{4} + \frac{1}{2}$	$\frac{d}{\pi} + \frac{-10\pi+8+\pi^2}{2\pi(-4+\pi)}$

F.5 Theorem 1, case 1b

$$\begin{aligned}
a_1 &= -1 + \frac{2}{d} + -\frac{4(-16\pi^2 + (-2 + \pi)(-6\pi^3 + 16\pi + 8\pi^2 + \pi^4) + 32\pi)}{\pi^3 d^2 (-2 + \pi)^2} + O(d^{-\frac{5}{2}}), \\
a_2 &= \frac{2}{d} + \frac{-2 + \frac{8}{\pi}}{d^2} + O(d^{-\frac{5}{2}}).
\end{aligned}$$

F.6 Eigenvalues

r-Representation	$\frac{(d-1)(d-2)}{2}$	$\frac{-2+\pi}{4\pi}$				
η -Representation	$\frac{d(d-3)}{2}$	$\frac{2+\pi}{4\pi}$				
Standard Representation	$d - 1$	0	$\frac{-2+\pi}{2\pi}$	$\frac{1}{4}$	$\frac{d}{4} + \frac{1}{2}$	
Trivial Representation	1	0	$\frac{d}{4} + \frac{-4+\pi+\pi^2}{2\pi(-4+\pi)}$	$\frac{d}{\pi} + \frac{-10\pi+8+\pi^2}{2\pi(-4+\pi)}$		

F.7 Theorem 1, case 3a

$$\begin{aligned}
a_1 &= 1 + \frac{16}{\pi d^2} + O\left(d^{-\frac{5}{2}}\right), \\
a_2 &= -\frac{8}{\pi d^2} + O\left(d^{-\frac{5}{2}}\right), \\
a_3 &= \frac{2}{d} + \frac{2(-8\pi^2 - \pi^3 - 16 + 4\pi)}{\pi^2 d^2 (2 + \pi)} + O\left(d^{-\frac{5}{2}}\right), \\
a_4 &= \frac{4}{\pi d} + \frac{32}{\pi^3 d^{\frac{3}{2}}} + \frac{4(-24\pi^4 - 160\pi^2 - \pi^5 + 256 + 192\pi + 28\pi^3)}{\pi^5 d^2 (2 + \pi)} + O\left(d^{-\frac{5}{2}}\right), \\
a_5 &= -1 + \frac{\frac{8}{\pi^2} + 2 + \frac{8}{\pi}}{d} + \frac{64(12 - \pi)}{3\pi^4 d^{\frac{3}{2}}(-2 + \pi)} \\
&\quad + \frac{2(-112\pi^5 - 3008\pi^2 - 240\pi^4 + 5120 + 2560\pi + \pi^8 + 8\sqrt{2}\pi^6 + 4\sqrt{2}\pi^7 + 672\pi^3 + 12\pi^7 + 104\pi^6)}{\pi^6 d^2 (4 - \pi^2)} \\
&\quad + O\left(d^{-\frac{5}{2}}\right), \\
a_6 &= \frac{2(-12\pi + 16 + \pi^3 + 4\pi^2)}{\pi^2 d (2 + \pi)} + \frac{16(-24\pi^2 + 64 + 24\pi + \pi^4 + 4\pi^3)}{\pi^4 d^{\frac{3}{2}}(4 + \pi^2 + 4\pi)} \\
&\quad + \frac{2\left(\begin{array}{c} -184\pi^7 - 26\pi^8 - 3968\pi^3 - 8192\pi^2 - 16\sqrt{2}\pi^7 - 4\sqrt{2}\pi^8 - 112\pi^5 - \pi^9 \\ -16\sqrt{2}\pi^6 + 20480 + 24576\pi + 864\pi^4 + 112\pi^6 \end{array}\right)}{\pi^6 d^2 (8 + \pi^3 + 12\pi + 6\pi^2)} + O\left(d^{-\frac{5}{2}}\right).
\end{aligned}$$

F.8 Eigenvalues

\mathfrak{r} -Representation	$\frac{(d-3)(d-4)}{2}$	$\frac{-2+\pi}{4\pi}$					
η -Representation	$\frac{(d-2)(d-5)}{2}$	$\frac{2+\pi}{4\pi}$					
Standard Representation $\mathfrak{5}_{d-2}$	$d-3$	0	$\frac{-2+\pi}{4\pi}$	$\frac{-2+\pi}{2\pi}$	$\frac{1}{4}$	$\frac{2+\pi}{4\pi}$	$\frac{d}{4} + \frac{1}{2}$
Standard Representation $\mathfrak{5}_2$	1	0	$\frac{-2+\pi}{4\pi}$	$\frac{-2+\pi}{2\pi}$	$\frac{1}{4}$	$\frac{d}{4} + \frac{1}{2}$	
Trivial Representation	1	0	0	$\frac{-2+\pi}{2\pi}$	$\frac{1}{4}$	$\frac{2+\pi}{4\pi}$	$\frac{d}{4} + \frac{-4+\pi+\pi^2}{-8\pi+2\pi^2}$
Tensor Representation $\mathfrak{5}_{d-2} \otimes \mathfrak{5}_2$	$d-3$	$\frac{d}{4} + \frac{1}{2}$	$\frac{-2+\pi}{4\pi}$	$\frac{2+\pi}{4\pi}$			

F.9 Identity

$$a_1 = 1, a_2 = 0.$$

F.10 Eigenvalues

\mathfrak{r} -Representation	$\frac{(d-1)(d-2)}{2}$	$\frac{-2+\pi}{4\pi}$				
η -Representation	$\frac{d(d-3)}{2}$	$\frac{2+\pi}{4\pi}$				
Standard Representation	$d-1$	0	$\frac{-2+\pi}{2\pi}$	$\frac{1}{4}$	$\frac{d}{4} + \frac{1}{2}$	
Trivial Representation	1	0	$\frac{d}{4} + \frac{-4+\pi+\pi^2}{2\pi(-4+\pi)}$	$\frac{d}{\pi} + \frac{-10\pi+8+\pi^2}{2\pi(-4+\pi)}$		

F.11 Theorem 1, case 3b

$$\begin{aligned}
a_1 &= -1 + \frac{2}{d} + \frac{-4 + \frac{24}{\pi}}{d^2} + O\left(d^{-\frac{5}{2}}\right), \\
a_2 &= \frac{2}{d} + \frac{-2 + \frac{12}{\pi}}{d^2} + O\left(d^{-\frac{5}{2}}\right), \\
a_3 &= \frac{8(-4\pi - \pi^2 + 8)}{\pi^2 d^2 (2 + \pi)} + O\left(d^{-\frac{5}{2}}\right), \\
a_4 &= \frac{2 - \frac{4}{\pi}}{d} + \frac{32(1 - \pi)}{\pi^3 d^{\frac{3}{2}}} + \frac{2(-344\pi^3 - \pi^6 - 512 + 4\pi^4 + 384\pi + 512\pi^2 + 26\pi^5)}{\pi^5 d^2 (2 + \pi)} + O\left(d^{-\frac{5}{2}}\right), \\
a_5 &= 1 + \frac{8(-1 + \pi)}{\pi^2 d} + \frac{8(-24\pi^3 - 200\pi + 96 + 3\pi^4 + 120\pi^2)}{3\pi^4 d^{\frac{3}{2}}(-2 + \pi)} \\
&\quad + \frac{2(-224\pi^6 - 6816\pi^3 - 496\pi^5 - 1088\pi^2 - \pi^8 - 5120 + 9728\pi + 52\pi^7 + 4112\pi^4)}{\pi^6 d^2 (4 - \pi^2)} + O\left(d^{-\frac{5}{2}}\right), \\
a_6 &= \frac{4(-\pi^2 - 8 + 6\pi)}{\pi^2 d (2 + \pi)} + \frac{16(-40\pi^2 - 40\pi - \pi^4 + 64 + 20\pi^3)}{\pi^4 d^{\frac{3}{2}}(4 + \pi^2 + 4\pi)} \\
&\quad + \frac{4(-4816\pi^4 - 116\pi^7 - 4544\pi^3 - 10240 + 4096\pi + 5\pi^8 + 14848\pi^2 + 176\pi^6 + 1632\pi^5)}{\pi^6 d^2 (8 + \pi^3 + 12\pi + 6\pi^2)} \\
&\quad + O\left(d^{-\frac{5}{2}}\right),
\end{aligned}$$

F.12 Eigenvalues

r-Representation	$\frac{(d-3)(d-4)}{2}$	$\frac{-2+\pi}{4\pi}$						
η -Representation	$\frac{(d-2)(d-5)}{2}$	$\frac{2+\pi}{4\pi}$						
Standard Representation \mathfrak{g}_{d-2}	$d-3$	0	$\frac{-2+\pi}{4\pi}$	$\frac{-2+\pi}{2\pi}$	$\frac{1}{4}$	$\frac{2+\pi}{4\pi}$	$\frac{d}{4} + \frac{1}{2}$	
Standard Representation \mathfrak{g}_2	1	0	$\frac{-2+\pi}{4\pi}$	$\frac{-2+\pi}{2\pi}$	$\frac{1}{4}$	$\frac{d}{4} + \frac{1}{2}$		
Trivial Representation	1	0	0	$\frac{-2+\pi}{2\pi}$	$\frac{1}{4}$	$\frac{2+\pi}{4\pi}$	$\frac{d}{4} + \frac{-4+\pi+\pi^2}{-8\pi+2\pi^2}$	
Tensor Representation $\mathfrak{g}_{d-2} \otimes \mathfrak{g}_2$	$d-3$	$\frac{d}{4} + \frac{1}{2}$	$\frac{-2+\pi}{4\pi}$	$\frac{2+\pi}{4\pi}$				

F.13 Theorem 1, case 4

$$\begin{aligned}
a_1 &= 1 + \frac{24}{\pi d^2} + O\left(d^{-\frac{5}{2}}\right), \\
a_2 &= -\frac{12}{\pi d^2} + O\left(d^{-\frac{5}{2}}\right), \\
a_3 &= \frac{2}{d} + \frac{2(-10\pi^2 - 32 - \pi^3 + 16\pi)}{\pi^2 d^2 (2 + \pi)} + O\left(d^{-\frac{5}{2}}\right), \\
a_4 &= \frac{4}{\pi d} + \frac{32}{\pi^3 d^{\frac{3}{2}}} + \frac{8(-17\pi^4 - 144\pi^2 - \pi^5 + 128 + 128\pi + 50\pi^3)}{\pi^5 d^2 (2 + \pi)} + O\left(d^{-\frac{5}{2}}\right), \\
a_5 &= -1 + \frac{\frac{8}{\pi^2} + 2 + \frac{8}{\pi}}{d} + \frac{64(12 - \pi)}{3\pi^4 d^{\frac{3}{2}}(-2 + \pi)} \\
&\quad + \frac{2(-288\pi^5 - 5056\pi^2 - 272\pi^4 + 5120 + \pi^8 + 3584\pi + 8\sqrt{3}\pi^6 + 4\sqrt{3}\pi^7 + 16\pi^7 + 1824\pi^3 + 144\pi^6)}{\pi^6 d^2 (4 - \pi^2)} \\
&\quad + O\left(d^{-\frac{5}{2}}\right), \\
a_6 &= \frac{2(-12\pi + 16 + \pi^3 + 4\pi^2)}{\pi^2 d (2 + \pi)} + \frac{16(-24\pi^2 + 64 + 24\pi + \pi^4 + 4\pi^3)}{\pi^4 d^{\frac{3}{2}}(4 + \pi^2 + 4\pi)} \\
&\quad + \frac{2\left(-1920\pi^5 - 164\pi^7 - 28\pi^8 - 4992\pi^3 - 13824\pi^2 - 16\sqrt{3}\pi^7 - 4\sqrt{3}\pi^8 - \pi^9\right)}{\pi^6 d^2 (8 + \pi^3 + 12\pi + 6\pi^2)} + O\left(d^{-\frac{5}{2}}\right).
\end{aligned}$$

F.14 Eigenvalues

\mathfrak{r}_{d-3} -Representation	$\frac{(d-5)(d-4)}{2}$	$\frac{-2+\pi}{4\pi}$						
\mathfrak{r}_3 -Representation	1	$\frac{-2+\pi}{4\pi}$						
η -Representation	$\frac{(d-3)(d-6)}{2}$	$\frac{2+\pi}{4\pi}$						
Standard Representation $\mathfrak{5}_{d-3}$	$d-4$	0	$\frac{-2+\pi}{4\pi}$	$\frac{-2+\pi}{2\pi}$	$\frac{1}{4}$	$\frac{2+\pi}{4\pi}$	$\frac{d}{4} + \frac{1}{2}$	
Standard Representation $\mathfrak{5}_3$	2	0	$\frac{-2+\pi}{4\pi}$	$\frac{-2+\pi}{2\pi}$	$\frac{1}{4}$	$\frac{d}{4} + \frac{1}{2}$		
Trivial Representation	1	0	0	$\frac{-2+\pi}{2\pi}$	$\frac{1}{4}$	$\frac{2+\pi}{4\pi}$	$\frac{d}{4} + \frac{-4+\pi+\pi^2}{-8\pi+2\pi^2}$	
Tensor Representation $\mathfrak{5}_{d-3} \otimes \mathfrak{5}_3$	$2d-8$	$\frac{d}{4} + \frac{1}{2}$	$\frac{-2+\pi}{4\pi}$	$\frac{2+\pi}{4\pi}$				